

MICROFICHE
RETAIN HARDCOPY

GRI

SAND94-1331

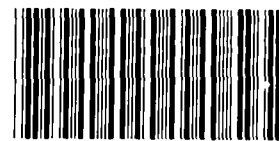
C.1

Annual Report

Development of Stimulation Diagnostic Technology

Prepared by:

Sandia National Laboratories



8665960

**SANDIA NATIONAL
LABORATORIES
TECHNICAL LIBRARY**

Gas Research Institute

Drilling and Completion Group

September 1994

vii, 56p.

DEVELOPMENT OF STIMULATION DIAGNOSTIC TECHNOLOGY

ANNUAL REPORT
(January 1993-December 1993)

Prepared by
N. R. Warpinski, J. C. Lorenz,
G. E. Sleaf, B. P. Engler
and R.S. Harding

Sandia National Laboratories
Division 6114
P.O. Box 5800
Albuquerque, New Mexico 87185

For
GAS RESEARCH INSTITUTE
Contract No. 5089-211-2059

GRI Project Manager
Steve Wolhart
Tight Gas Sands Field Evaluation

February 1994

REPORT DOCUMENTATION PAGE		1. REPORT NO. GRI-94/0150	2.	3. Recipient's Accession No.
4. Title and Subtitle DEVELOPMENT OF STIMULATION DIAGNOSTIC TECHNOLOGY			5. Report Date 6/1/93 Preparation	
			6.	
7. Author(s) N.R. Warpinski, J.C. Lorenz, G.E. Sleaf, B.P. Engler & R.S. Harding			8. Performing Organization Rept. No. SAND94-1331	
9. Performing Organization Name and Address Sandia National Laboratories Division 6114 P.O. Box 5800 Albuquerque, New Mexico 87185			10. Project/Task/Work Unit No.	
			11. Contract(C) or Grant(G) No. (C) 5089-211-2059 (G)	
12. Sponsoring Organization Name and Address Gas Research Institute 8600 Bryn Mawr Avenue Chicago, Illinois 60631			13. Type of Report & Period Covered 1993 Annual Report,	
			14.	
15. Supplementary Notes				
16. Abstract (Limit: 200 words) <p>The approach to stimulation diagnostics is to integrate in situ stress measurements (including microfracs, anelastic strain recovery, circumferential velocity analysis, and coring-induced fractures) with natural fracture characterization, stimulation analyses (including FRACPRO™, other models, finite-element analyses, and various pressure analyses), and fracture diagnostics in order to validate hydraulic fracture concepts, models and diagnostic capabilities. While the emphasis for the last year was on fracture diagnostics, there has also been considerable work on natural fractures in the Green River basin and core-based stress measurements. Studies of outcrop and core have shown a consistent, rational pattern to natural fracture development in the basin, and two topical reports detailing these results have been initiated. Similarly, a topical report on core-based stress measurements and a more general stress-azimuth report have been completed. In the stimulation area, a topical report on the entire fracture-modeling forum data set has been completed. An advanced diagnostics program was initiated in the last quarter of 1993, and excellent results were obtained in a field diagnostic experiment at M-Site. Diagnostics were obtained using advanced multi-level receivers during four separate fracture treatments, and preliminary analysis of these results have successfully mapped out the fracture extent. In addition, a velocity survey was conducted to aid in location analyses, and treatment-well diagnostics were conducted during two of the treatments.</p>				
17. Document Analysis a. Descriptors <p>Tight gas sands, in situ stress, stress measurement, natural fractures, Green River basin, hydraulic fracturing, fracture diagnostics</p> <p>b. Identifiers/Open-Ended Terms</p> <p>anelastic strain recovery, circumferential velocity anisotropy, coring induced fractures, natural fractures, Green River basin, stimulation, hydraulic-fracture diagnostics, microseisms, seismic analysis.</p> <p>c. COSATI Field/Group</p>				
18. Availability Statement Release unlimited		19. Security Class (This Report)		21. No. of Pages
		20. Security Class (This Page) unclassified		22. Price

GRI DISCLAIMER

LEGAL NOTICE This report was prepared by Sandia National Laboratories as an account of work sponsored by the Gas Research Institute (GRI). Neither GRI, members of GRI, nor any person acting on behalf of either:

- a. Makes any warranty or representation, express or implied, with respect to the accuracy, completeness, or usefulness of the information contained in this report, or that the use of any apparatus, method, or process disclosed in this report may not infringe privately owned rights; or
- b. Assumes any liability with respect to the use of, or for damages resulting from the use of, any information, apparatus, method, or process disclosed in this report.

Title	Development of Stimulation Diagnostic Technology
Contractor	Sandia National Laboratories
	GRI Contract Number: 5089-211-2059
Principal Investigator	N. R. Warpinski
Report Period	January 1993-December 1993 Annual Report
Objective	To apply Sandia's expertise and technology towards the development of stimulation diagnostic technology in the areas of in situ stress, natural fracturing, stimulation processes and instrumentation systems.
Technical Perspective	Large quantities of natural gas exist in low permeability reservoirs throughout the US. Characteristics of these reservoirs, however, make production difficult and often uneconomic. Matrix rock permeabilities are often submicrodarcy, and natural fractures are commonly marginal, being anisotropic and easily damaged. Stimulation is required for these types of reservoirs, with hydraulic fracturing being the primary stimulation option. Understanding stimulation behavior is difficult, however, because of the complex nature of most of these reservoirs. Diagnostics that can map out the fracture length, height, and azimuth are the missing element in hydraulic-fracture analysis. Integrating knowledge of the matrix rock, natural fractures, in situ stresses with stimulation models and diagnostics is required if stimulation effectiveness is to be determined and enhanced.
Results	While the emphasis for the last year was on fracture diagnostics, there has also been considerable work on natural fractures in the Green River basin and core-based stress measurements. Studies of outcrop and core have shown a consistent, rational pattern to natural fracture development in the basin, and two topical reports detailing these results have been initiated. Similarly, a topical report on core-based stress measurements and a more general stress-azimuth report have been completed. In the stimulation area, a topical report on the entire fracture-modeling forum data set has been completed. An advanced diagnostics program was

initiated in the last quarter of 1993, and excellent results were obtained in a field diagnostic experiment at M-Site. Diagnostics were obtained using advanced multi-level receivers during four separate fracture treatments, and preliminary analysis of these results have successfully mapped out the fracture extent. In addition, a velocity survey was conducted to aid in location analyses, and treatment-well diagnostics were conducted during two of the treatments.

integrate	Technical	The approach to stimulation diagnostics is to
	Approach	in situ stress measurements (including microfracs, anelastic strain recovery, circumferential velocity analysis, and coring-induced fractures) with natural fracture characterization, stimulation analyses (including Fracpro, other models, finite-element analyses, and various pressure analyses), and fracture diagnostics in order to validate hydraulic fracture concepts, models and diagnostic capabilities. In the next two years, the emphasis will be on developing a fracture-diagnostics system to map out hydraulic-fracture length and other parameters. The ultimate goal is to develop a real-time, industry-run, fracture-diagnostics capability.
	Project difficult to Implication	Hydraulic fracturing is a complex process and is optimize. This project combines reservoir characterization, fracture diagnostics and stimulation analyses to better understand hydraulic fracturing. The missing element, as noted above, is the ability to accurately measure fracture dimensions including length in a practical manner. Significant progress was made toward developing this capability in the past year and this will continue to be the major emphasis of this project. Other key results from this project include the characterization of natural fractures in the Green River Basin, a comparison of fracture models using SFE No. 3 data and a catalog of core-based stress measurement techniques. These results, combined with fracture diagnostics and other stimulation analyses, will help to optimize the process of hydraulic fracturing.

Steve Wolhart
Technology Manager, Drilling & Completion

TABLE OF CONTENTS

1.0	RESEARCH OBJECTIVES	1
2.0	SUMMARY OF ALL PREVIOUS WORK PERFORMED	3
3.0	SPECIFIC OBJECTIVES OF THE CURRENT YEAR	4
4.0	WORK PLANS FOR THE CURRENT YEAR	5
5.0	IN SITU STRESS	6
6.0	NATURAL FRACTURES	9
7.0	STIMULATION	14
8.0	M-SITE EXPERIMENT	15
9.0	OTHER DIAGNOSTIC TASKS	25
10.0	REFERENCES	26
11.0	MAJOR ACHIEVEMENTS	27
12.0	MAJOR PROBLEMS	28
13.0	CONCLUSIONS	29
14.0	OBJECTIVES AND WORK PLANNED FOR NEXT YEAR	30

Tables

Table 1. Orientation scan azimuths, 1993 M-Site Test

Figure Captions

- Figure 1. Field data from sample #1, Amoco well.
- Figure 2. Usable horizontal strain data from sample #1, Amoco well.
- Figure 3. Corrected horizontal strain data from sample #1, Amoco well.
- Figure 4. Relative azimuth results from sample #1, Amoco well.
- Figure 5. Field data from sample #3, Amoco well.
- Figure 6. Usable strain data from sample #3, Amoco well.
- Figure 7. Corrected horizontal strain data from sample #3, Amoco well.
- Figure 8. North-south striking J1 fractures
- Figure 9. East-west striking J2 fractures superimposed on J1 fractures
- Figure 10. Irregular J3 fractures at a structural discontinuity along the thrust plate that forms the Hogsback
- Figure 11. Current layout of M-Site experiment
- Figure 12. Noise limits of borehole seismic sensors.
- Figure 13. Schematic layout of crosswell velocity survey.
- Figure 14. Common receiver gather of raw signals.
- Figure 15. Common receiver gather of filtered data.
- Figure 16. Example orientation data for level 1, shot at 4930 ft.
- Figure 17. Example orientation data for level 2, shot at 4930 ft.
- Figure 18. Example orientation data for level 3, shot at 4930 ft.
- Figure 19. Example orientation data for level 4, shot at 4930 ft.
- Figure 20. Orientation results for all levels.
- Figure 21. Example microseism data for level 1, microseism #20, frac #1.
- Figure 22. Example microseism data for level 2, microseism #20, frac #1.
- Figure 23. Example microseism data for level 3, microseism #20, frac #1.
- Figure 24. Example microseism data for level 4, microseism #20, frac #1.
- Figure 25. Initial map and histogram of frac #1 using unfiltered microseism data.

1.0 RESEARCH OBJECTIVES

The objective of this project is for Sandia National Laboratories to apply its expertise and technology towards the development of stimulation diagnostic technology. Stimulation diagnostic technology, as defined here, contains different areas such as (1) in situ stresses, (2) natural fracture characterization, (3) stimulation modeling, (4) hydraulic-fracture diagnostics, and (5) the design and conduct of field experiments. Integration of these areas can yield a more complete analysis of hydraulic fracture behavior and effectiveness in the reservoir. Beginning in the last quarter of this year, additional efforts were initiated to develop microseismic fracture diagnostics into a reliable, accurate, near-real time service.

In situ stresses, both the direction and the magnitudes, are of vital importance to the production of gas from low permeability reservoirs. Stress data are required for advanced design and analysis of fracture treatments, for completion information, and for understanding of the production mechanisms in tight reservoirs. The specific objective of the in situ stress task is to integrate core, log, and injection stress data into a complete picture of the stress in the reservoir, and to develop a "catalog" of techniques, each with a set of validated procedures, which can be brought to bear on the problem of stress determination.

Many of the tight reservoirs in the US, particularly in western basins, produce primarily from marginal natural fracture systems. Understanding the natural fracture system and the effects of stress, pore pressure, water saturation, etc. are important for any rational decisions on completion and stimulation of wells in these reservoirs. The specific objectives of the natural fracture task are to obtain description and distributions of the fracture systems from core, logs and outcrops, determine the importance of the fracture systems, and integrate these data for use in completion/stimulation design and production operations.

Effective hydraulic fracture stimulation requires a comprehensive design model that can adequately predict fracture behavior and reservoir performance. GRI has such a model (Fracpro) that can be used for design, analysis, and real-time control. Confident use of such models requires validation in realistic physical situations, a difficult task since the created fractures are not very accessible. The specific objectives of the stimulation modeling task are to perform analyses of injections using pressure analyses, finite element models, simple fracture models, and other resources in order to obtain a comparison with Fracpro and to aid in its validation.

Information on fracture behavior is currently available only through the use of indirect fracture diagnostic techniques, but these techniques are far from being routine field procedures, nor do they have the universal confidence of industry. The advancement of microseismic (and other seismic) monitoring requires rigorous standards for receivers, recorders, and processing algorithms. Completion of this task requires the application of advanced multi-station receivers that can faithfully record the particle motion induced by the specific events, the use of telemetry and recorders with sufficient dynamic range and band width to transmit and store the data, and the development of analysis techniques that can be applied in real-time or near-real-time modes.

Field experiments are an integral part of GRI's Stimulation & Completion Project and the means by which models, diagnostics, and other procedures can be tested, refined, and verified. Sandia has a lead role in the diagnostic phases of the M-Site tests that are being conducted in the Piceance basin near Rifle, CO. This work includes the design of the instrumentation string of accelerometers and tiltmeters for a newly drilled monitor well and the application of wireline microseismic instrumentation for existing wells. These field experiments will provide the baseline information for developing the hardware and processing algorithms for fracture diagnostic analysis.

2.0 SUMMARY OF ALL PREVIOUS WORK PERFORMED

2.1 In Situ Stress

Previous work on in situ stresses includes ASR analyses of SFE-4, Canyon Sands, and UPRC Frontier core, and Circumferential Velocity analyses of the same core plus Maxus Cleveland formation and Berea core. These results were important source material for the core-based stress measurement report completed this year.

2.2 Natural Fractures

Previous natural fracture studies include Green River basin fieldwork which identified two primary fracture sets and efforts to reconstruct the tectonic development of the basin which led to the development of the fractures. Studies of natural fractures in core were used to develop a theory of the role of diagenesis in fracture development. This theory has proved useful in explaining Frontier fracture systems.

2.3 Stimulation

Previous stimulation activities include most importantly the analysis and documentation of the Fracture Propagation Modeling Forum results. These data were included in an SPE paper summarizing the results. Other modeling activities have been conducted to assess site suitability.

2.4 Diagnostics

A considerable effort in fracture diagnostics was conducted in 1992 at the M-Site during the site suitability testing. A single advanced seismic receiver was fielded in an offset well and captured microseisms generated during four fracture treatments. These results showed that the current M-Site is an excellent location for this research.

3.0 SPECIFIC OBJECTIVES OF THE CURRENT YEAR

Specific objectives of the current year are:

Continue the evaluation of stress measurement techniques, leading to an understanding of the potential of these techniques, including their accuracy, reliability, problem areas, and other important features.

Continue the natural fracture studies of the Frontier formation in the Green River basin, with particular emphasis on the Moxa Arch area, in order to develop an understanding of the natural fractures within this basin, their development, and their potential for gas production.

Provide stimulation analyses of hydraulic fractures as appropriate to GRI's objectives on specific tests.

Complete work on the M-Site suitability test, with particular reference as to the suitability of the site for continuing diagnostic work.

Design and begin full-scale diagnostic tests at the M-Site for the purpose of laying the groundwork for developing a fracture diagnostic service industry.

4.0 WORK PLANS FOR THE CURRENT YEAR

Complete a core-based stress report and a stress azimuth report.

Perform stress measurements in any appropriate industry wells where research information could be gained.

Complete a topical report on natural fractures in the Frontier formation of the Green River basin, based on field outcrop studies and any available core data.

Continue Green River basin field studies and perform fracture examination studies in any appropriate industry wells where additional fracture information could be obtained.

Complete the topical report detailing all of the modeling data from the Hydraulic Fracture Propagation Modeling Forum.

Complete analysis of the microseismic data from the M-Site suitability test.

Design and conduct a multi-level diagnostics field experiment in the A sand at M-Site.

Begin design studies for a monitor well at M-Site.

5.0 IN SITU STRESS

Knowledge of the directions and magnitudes of in situ stress are of vital importance to the production of gas from low permeability reservoirs. Stress data are used in the design and analysis of hydraulic fracture stimulations and are necessary for the understanding of parameters affecting production. However, in situ stresses are difficult to measure, and there is no commonly accepted practice for determining the stresses. As a result, there is often a lack of confidence in stress data from any one technique. In light of this reality, it is common sense to develop as many ways as possible to determine stress parameters.

Sandia is currently working on integrating information from anelastic strain recovery (ASR), differential strain curve analysis (DSCA), circumferential velocity anisotropy (CVA), coring-induced fractures, log-derived wellbore effects, overcoring of archived core and microfrac stress measurements in order to obtain an integrated program to provide the best possible stress measurement.

5.1 Preparation of Topical Reports on Core-Based Stress Measurements

During 1993, a topical report on core-based stress measurements was prepared and published (GRI-93/0270). The title of this report is *Core Based Stress Measurements: A Guide to Their Application*.¹ Excerpts from this report were then used for a second, joint CER/Sandia topical report on stress azimuth measurements, *Techniques for Determining Subsurface Stress Direction and Assessing Hydraulic Fracture Azimuth* (GRI-93/0429).

The report on core-based stress measurements considered circumferential velocity anisotropy (CVA), petrographic examination of microcracks, anelastic strain recovery (ASR), overcoring of archived core, differential strain curve analysis (DSCA) and differential wave velocity analysis (DWVA), examination of coring induced fractures, and measurements of the Kaiser effect. In each case, the concept was discussed first, followed by data acquisition techniques, data analysis (including problems and limitations), example applications, and a general discussion of the technique, its value and its advantages.

5.2 Support for Amoco Production Company's Green River Basin Play

ASR measurements were performed on three cores from an Amoco well in the Green River basin. While the initial field examination of these tests were negative, as the rock behavior appeared to be due to thermal strains, some additional analysis shows that the results from two cores are acceptable. This data set is an excellent example of the effects of thermal strains on ASR data. More importantly, it is a good example of the procedures that can be taken to correct the data (subtract thermal strains).

5.2.1 Data

Although data were taken on three cores, only two of the cores had usable results on all three horizontal gages. The field data from sample #1 are shown in Figure 1. The axial gage is not functioning properly, but it is not needed for azimuth determination. The usable horizontal strain data are extracted and shown in Figure 2. All three horizontal gages are influenced by the temperature fluctuations, and the overall field impression was that most of the strain recovery was thermally induced.

A simple thermal correction can be made by

$$\epsilon_i^c = \epsilon_i - 6(T_i - T_o) .$$

The superscript c refers to corrected strain data, T_i refers to the temperature at any time, T_o refers to the temperature at zero time, and 6 is a typical coefficient of thermal expansion in microstrains/degree F. This crude correction ignores the fact that the temperature has not equilibrated throughout the sample, but it does often eliminate the major effects of temperature. Figure 3 shows the resultant curves when this correction is made. The data now look like typical ASR results (the contractions occur frequently in tight rocks and are due to a slow bleed-off of pore pressure), and can be quickly analyzed for azimuth, as shown in Figure 4. In this case the azimuth is stable with time, which suggests that the ASR results are reasonably good. This figure shows the estimated time-scale for the full recovery process and where these ASR data fit within the process. The final relative azimuth is 61° counterclockwise from the PSL. This number is used for the stress azimuth estimate.

The field data from sample #3 are shown in Figure 5, the extracted strains are given in Figure 6, and the temperature corrected strains are given in Figure 7. These results are still contracting and diverging, suggesting that the ASR process is still occurring when the gages were turned off. The azimuth data are not constant, but rather show a consistent change. Such a change should not be occurring in a homogeneous isotropic rock (of, course, such rocks do not exist in nature), so these results are not considered as reliable as sample #1.

The final relative azimuth is -79° (or +101°), but it is continuing to decrease up to the point where the gages were turned off. An estimate of the final azimuth is more likely -90° (which is equivalent to +90°). Thus, the results from this gage are 29° - 40° different from sample #1 (there is a similar PSL for both samples).

Finally, the axial strains are intermediate to the horizontal strains, suggesting that the overburden stress is the intermediate stress, i.e., one of the horizontal stresses is greater than the overburden. However, this inference may be skewed by the effects of the shale laminations on the axial gage.

Although sample #2 is not usable because one of the horizontal gages did not respond, a quick check of the two functioning gages show that the response is similar to sample #1. In both cases the 45° gage has a strain recovery that is slightly greater than the strain from the 90° gage. This information cannot be used for stress azimuth (three gages are needed), but it supports the results from sample #1.

5.2.2 Conclusion

Two of the ASR samples show reasonably good strain relaxation behavior, and the results from those two tests were used for azimuth estimates (absolute orientation data can not be given at this time). The uncertainty is probably $\pm 20^\circ$. These results indicate that thermal corrections are an important part of the analysis of ASR data, and such corrections should be employed whenever temperature variations exceed about 2° F.

5.3 Frontier formation stress data

Information from GRI Frontier formation stress tests were presented at a Green River basin workshop in Denver, on April 25, 1993. This workshop was associated with the SPE Rocky Mt. Regional /Low Permeability Symposium and included information on geology, natural fractures, in situ stresses, logging, stimulation, testing and production. Information provided by Sandia included stress data obtained from microfracs, ASR, coring-induced fractures, velocity anisotropy, and other tests.

6.0 NATURAL FRACTURES

Many of the tight sandstones, particularly those in western US basins, have matrix permeabilities of a few microdarcies or less. Economic production from such reservoirs is impossible unless natural fractures or other mechanisms provide additional permeability. Well testing of many of these microdarcy or submicrodarcy reservoirs often yields effective permeabilities of tens or hundreds of microdarcies, substantiating the hypothesis that most of these reservoirs are fractured. Outcrop, log and core studies have also shown the presence of natural fractures. Knowledge of the characteristics and importance of the natural fractures is important because it may affect the stimulation or other completion plan.

6.1 Natural Fractures in Outcrop of the Frontier Formation Sandstones near Kemmerer, WY

Three categories of bed-normal, natural extension fractures were documented in the sandstones of the Frontier Formation exposed along the Oyster Ridge Hogsback in southwestern Wyoming. The first set of fractures (J1) formed during basin subsidence prior to thrusting, and strikes generally north-south parallel to the basin axis, sub-parallel to the present-day ridge. The second group of fractures (J2) formed as a result of north-south dilatancy during early stages of thrusting, and trends approximately normal to the ridge. Structures such as tear faults and lateral ramps within the thrust plate produced a third group of localized fractures (J3) with strikes that vary significantly from location to location.

1. J1 fractures (oldest) comprise a throughgoing, regional set of extension fractures, created during basin subsidence and Laramide thrusting. The average strike is about 350 to 10 degrees. Fractures commonly extend the length of an outcrop, as shown in Figure 8.
2. J2 fractures are extension fractures related to north-south stretching and dilatancy during Sevier thrusting. They commonly trend nearly normal to the local strike of bedding and therefore strike within 30 degrees of east-west, as seen in Figure 9. They may either cut across or terminate against J1 fractures, and therefore may be either short or long in average length depending on locality.
3. J3 fractures are the youngest, and consist of local sub-group sets of extension fractures related to local structures along the thrust plate as shown in Figure 10. They have no characteristic regional strike or dimensions.

Temporal overlap in the formation of groups 2 and 3 may have occurred locally, and creates ambiguity in the interpretations of these two groups.

The north-striking J1 fractures predate thrusting, translation, and folding, and thus did not originate as extension fractures produced during folding, nor by flexure at hinges of large-scale folds. A plausible loading history that accounts for J1 fracture development prior to thrusting is as follows: as the basin subsided during latest Cretaceous and early Tertiary time, strata could have been stretched east-west due to lengthening parallel to bedding, since the original nearly-flat depositional surface had to conform to the asymmetric basin profile during burial. Concurrent indentation of the Wind River Mountains and the Uinta mountains from the north and south respectively would have enhanced the horizontal stress anisotropy and the fracture potential of the strata at this time.

J2 fractures post-date J1 fractures. They also predate J3 fractures, although the J2-J3 geometries are locally suggestive of interaction. J2 fractures formed just prior to or during the early stages of thrusting. East-directed tectonic shortening is inferred to have produced north-south extension, especially in the area of the foreland adjacent to a convex salient of the thrust belt, accounting for J2 fractures.

J3 fractures are the youngest fractures, and the sub-sets of this group have no consistent orientation or characteristics along the length of the Hogsback. However, the apparent correlation of J3 fractures with transverse structures within the thrust constitutes strong evidence for an origin during thrusting, translation, and folding. Thus, these fractures are interpreted to have formed due to local structural and spatial accommodations along the thrust plate during thrusting, and soon after, or even locally contemporaneously with, the formation of J2 fractures.

In extrapolating these fracture patterns eastward into the subsurface, the J1 fractures are inferred to be widespread within the confines of the foredeep west of the Moxa arch, and possibly eastward throughout the basin depending on the degree of influence of the Laramide uplifts north and south of the basin. In the basin, however, J1 fracture development and orientation may vary depending on local structures and the relative magnitudes of locally-created stresses.

J2 fractures are the product of thin-skinned thrusting, and the stresses imparted to the undeformed strata east of the thrust belt dissipated rapidly away from the thrust front. The J2 fracture pattern is expected to be most prominent only within the thrust belt and immediately east of it. Similarly, the J3 fractures will be localized within transverse structures along thrust plates, and can not be extrapolated eastward into the deep basin.

6.2 Lithologic Controls on Fracturing

Adjacent sandstone beds within the Frontier Formation locally may contain dissimilar fracture sets. Bed thickness, structural context, and depositional environment have been considered as possible controlling factors, but none of these factors present consistent relationships with the varying fracture orientations.

However, a plausible relationship exists between fracture orientation and the petrophysical properties of the rock, properties which controlled the susceptibility of the rock to fracturing through time, and which are in turn a product of its composition and diagenetic history. Petrologic study shows that similar characteristics in different depositional facies resulted from parallel diagenetic sequences. On the other hand, in several cases different diagenetic sequences apparently produced similar rock properties, and hence similar fracture characteristics within otherwise disparate rocks.

Outcrop examination suggested that there are four basic fracture facies in the sandstones. These are:

1. beds containing J1 fractures
2. beds containing J2 fractures
3. beds containing both sets of fractures
4. beds without significant fracturing

The most important variable within the samples collected seems to be the diagenetic sequence, including several types and episodes of cementation and dissolution. However, matrix material such as clays and organic components that were introduced during initial deposition are also contributing factors to the variability in mechanical properties.

Rocks containing primarily J1 fractures consistently exhibit 1) evidence for early quartz cementation by silica overgrowths on quartz grains and 2) later dissolution of much of the silica phase. This has resulted in a relatively high-porosity rock. In contrast to other fracture facies, there is little evidence for a later calcite cementation phase within rocks of this group. This is not a surficial weathering effect since the etching of quartz grains that is commonly associated with later calcite cementation in other rocks is not present, and because this facies is also recognized in sandstone core from the subsurface.

This observation is consistent with the proposed origin of the J1 fractures early in the history of the strata. Early silica cementation would have created brittle properties in the rocks, making them susceptible to fracturing contemporaneously with east-west extension of the strata during subsidence, and thus creating an essentially north-south fracture set.

Later dissolution of much of the early silica, combined with the absence of the subsequent calcite cementation phase, resulted in relative ductility of the rocks at a later time. The absence of the younger, northeast-trending J2 fracture set in these strata may then be attributed to more ductile properties during later, thrust-related stress events.

Rocks containing only J2 fractures display the inverse diagenetic sequence, having little or no evidence for early silica cement but commonly containing significant amounts of later calcite cement. Calcite fills most of the porosity of these samples. Thus these samples are inferred to have been poorly cemented and relatively ductile during the stress phase which resulted in J1 fractures in most of the rocks, yet they were brittle and susceptible to fracturing during the later stress episodes that produced J2 fractures.

A third facies characteristically contains both J1 and J2 fractures. Samples from this facies typically display both early quartz and later calcite cements (separated by the silica dissolution phase). These samples are inferred to have been brittle due to cementation during both loading events. These rocks also have relatively low porosity.

Depositional environment may have influenced the diagenetic sequence to a degree; samples with both J1 and J2 fractures are commonly from cleaner depositional facies such as hummocky cross-stratified shallow marine/lower shoreface sandstones where clays were rarely deposited. However, the sands include significant amounts of rock fragments and were never clean orthoquartzites.

Fracture facies 4 is characterized by the general absence of fractures in outcrop, and includes rocks from a diversity of depositional facies. Notably, it includes sandstones that were initially deposited in the same environment as the hummocky strata noted in group 3, but which were subsequently intensely burrowed. Bioturbation mixed a significant percentage of rock fragments, organic material, and detrital clay into the resulting rock. This facies also includes thick, white, amorphous sandstones believed to be upper shoreface deposits. The porosity of these samples ranges from very low to very high.

The absence of fractures suggests that the rocks were relatively ductile. The ductility of some of these samples derives from the mixture of clay and organic material into the sandstone, whereas in others it may be due to a high percentage of ductile rock fragments that comprise the sand fraction. In still another example, ductility may be attributed to a very high porosity (30%), and the resulting limited grain to grain contact. Thus there were several diagenetic and/or depositional facies that produced rock properties that were not susceptible to fracturing, although these strata account for only a small percentage of the Frontier Formation.

The presence of different fracture facies in Frontier sandstones adds another level to the known heterogeneity of these reservoirs. It is usually accepted that primary sedimentary/diagenetic heterogeneity controls matrix permeability distributions (i.e., shale breaks in a sandstone are barriers to gas flow). It is also reasonably well understood that this heterogeneity in turn controls the distribution of natural-fracture permeability (i.e., fractures terminate at shale breaks, and therefore fracture permeability is also limited by such reservoir heterogeneities). The above observations on fracture facies suggest that the sedimentary and diagenetic history of the strata may also control 1) the likelihood of a particular sandstone facies being fractured, and 2) the orientation of the fractures expected.

6.3 Observations on Fractures in Core from the Frewen Deep #4 well

Core from the Frontier Sandstone at a depth of approximately 18,300 ft from Amoco's Frewen Deep #4 well in the eastern Green River basin was examined, and found to contain numerous natural and coring-induced petal fractures. The dominant set of natural fractures is mineralized to partially mineralized with locally significant remnant porosity. These fractures maintain a consistent, near-normal strike relationship to the petal fractures, indicating a rotation of the maximum in situ compressive stress by 70-90 degrees since initial fracturing. Thus the present stress orientation would act to keep the fracture permeability to a minimum despite the obvious remnant porosity. Paleomagnetic orientation of the core indicates that the natural fractures are oriented nearly east-west, and the present-day stress, indicated by the petal fracture strike, is north-northwest.

Residual bitumen (cooked-out oil) lines the walls of many of the fractures, and highlights what appear to be unmineralized, fracture-termination process zones. This solid residue is undoubtedly detrimental to the fracture permeability.

The sequence of geologic events recorded in this core is interpreted to consist of (1) natural fracturing, (2) hydrocarbon overmaturation, (3) secondary, near-parallel natural fracturing, (4) vertical compression resulting in horizontal stylolites, (5) re-orientation of the horizontal stresses by nearly 90 degrees to the present orientation, and (6) associated minor fracturing under this stress regime.

The numerically dominant fracture set (up to ten fractures noted in the 86 ft of core studied), consists of partially to completely calcite-mineralized, vertical and near-vertical fractures. Mineralized fracture widths up to 0.5 mm are common, locally with up to 50% of the width consisting of open porosity. These fractures maintain a relatively consistent 80-110 degree angular relationship to the petal fractures.

These fractures are lithologically confined to sandstones, commonly terminating at bedding discontinuities. Locally the bedding planes have been stylolitized, indicating vertical compression and dissolution of rock along the horizontal plane. Some of the fractures terminate at the dissolution planes, with indications that the fracture formed before, and was subject to, that same dissolution.

Two secondary fracture sets are present in this core. One set is only ambiguously distinguished from the dominant set by an oblique strike of up to 20 degrees to the dominant fractures, and by the absence of associated bitumen. In one case, a fracture of the dominant set is offset along bedding planes whereas the adjacent fracture of the sub-parallel secondary set is not, indicating a relative age relationship of 1) dominant fracture, 2) bedding plane offset, and 3) secondary fracture.

The other set of secondary natural fractures is represented in the core by two small, mineralized fractures that strike parallel to the petal fractures. One of these fractures intersects a dominant fracture at nearly right angles. Since these two secondary fractures parallel the present-day horizontal stress, they are inferred to be the youngest fractures. They are significantly smaller and less common than fractures of the dominant set. However, the degree of influence of this set of fractures on reservoir permeability system cannot be determined since the fractures were noted only in the seven ft of core butts examined; it is possible that examination of the rest of the core butts might reveal a slightly larger population.

6.4 Support for Amoco Production Company's Green River Basin Play

Amoco Production Company is developing a horizontal gas play in the Almond Formation in the eastern Green River basin. Based on recommendations from Sandia, Amoco has drilled two deviated pilot holes in order to assess the natural fracture characteristics of the formation. Sandia has been on site to evaluate core. A lateral was drilled and cored at these sites, along the azimuth dictated by the data from the pilot hole.

7.0 STIMULATION

Some form of stimulation, usually hydraulic fracturing, is required for the economic production of gas from tight reservoirs. A long-sought objective has been comprehensive hydraulic-fracture models that could be used for the design, analysis, and, ultimately, real-time control of the fracturing process. In order to help validate such comprehensive models, Sandia is tasked to (1) analyze appropriate field stimulation and minifrac data in order to obtain an independent assessment of fracture performance, and (2) conduct any advanced activities (e.g., finite element analyses, model comparisons, etc.) which provide independent confirmation of model validity.

The primary activity of this task for 1993 was the compilation of the complete set of results of the Fracture Modeling Propagation Forum, and the preparation and publication of a topical report (GRI-93/0109) detailing these results. The title of this report is *Hydraulic Fracture Model Comparison Study: Complete Results*.² While the original SPE paper on these results presented primarily the data at the end of pumping, the topical report gives all of the data throughout the treatments, in $1/8$ time increments. In addition, Appendices give many other results presented by the authors, including width profiles as a function of time.

In addition to the topical report, the SPE paper on these data was accepted for publication in the February, 1994 issue of *SPE Production and Facilities*.

8.0 M-SITE EXPERIMENT

Three of the primary goals of GRI's Stimulation and Completion program are (1) validation of hydraulic-fracture design models, (2) development of hydraulic-fracture length diagnostics, and (3) validation of all fracture-diagnostic technology. Validation implies a confirmation of the predicted results by actual measurement in the field, and thus requires an instrumented facility where fracture behavior can be measured. The effort to develop such a capability is named the M-Site Experiments. Sandia has been involved (along with CER Corp. and RES) in the development and testing at M-Site.

The M-Site location is in the Piceance basin near the town of Rifle, CO, in Mesaverde sandstones at depths from 4000-5000 ft. Two wells, designated MWX-2 and MWX-3, are currently available for testing and fracturing and are shown in Figure 11. During the fall of 1992, a site suitability test was conducted, from which highly positive results were obtained. During 1993, the first of several experiments was conducted in the A sand, and planning for a new monitor well was initiated.

8.1 M-Site Suitability Test

Analysis of the M-Site suitability test, conducted in the fall of 1992, was completed in 1993 with the preparation of a topical report titled *Multi-Site Project Seismic Verification Experiment and Assessment of Site Suitability*³ (GRI-93/0050, authors from CER Corp. and Sandia) and a SPE paper titled *The Use of Broadband Microseisms for Hydraulic Fracture Mapping*⁴ (SPE 26485, authors G.E. Sleefe, N.R. Warpinski, B.P. Engler). The topical report provides all of the information obtained during the suitability test and the SPE paper discusses in depth the requirements for performing accurate reliable fracture mapping using the microseismic technique. Of particular importance are some of the requirements for obtaining accurate microseismic data.

8.1.1 Need for Advanced Seismic Receiver

In order to utilize the polarization approach for event mapping, the seismic receiver instrument must faithfully record the particle motion of the seismic wave-field that is incident on the borehole. The conventional wall-locking geophone instrument generally does not enable the accurate measurement of particle motion over a wide frequency range. Two instrument limitations can cause the wall-locked geophone to record inaccurate particle motions. The first limitation, known as locking resonance, results from inadequate coupling of the geophones to the borehole over a wide frequency band.⁵ When the locking arm of the instrument extends to clamp the unit to the borehole, the geophones are coupled to the borehole only at relatively low frequencies. At some higher frequency, the motions of the clamping unit do not follow the motions of the borehole wall. In conventional VSP geophone receivers, the resonant frequency of the clamped receiver is typically in the 200 Hz to 400 Hz range. Therefore, conventional VSP instruments can only be used for accurate polarization measurements for seismic excitations below about 200 Hz. In order to extend the frequency range above this limit, one must either use a novel clamping package or cement the geophones directly into the formation.

The second limitation in using the polarization method is that the geophone itself often does not accurately measure particle motion over a wide frequency range. Conventional geophones exhibit spurious modes which are due to off-axis excitation of the geophone springs.⁶ The spurious mode manifests itself as a resonance effect which occurs at a frequency which is approximately 25 times higher than the natural frequency of the geophone. For example, a 10 Hz geophone can exhibit spurious modes at and above 250 Hz, thus limiting its usefulness above 250 Hz. Additionally, the low frequency end of the geophone does not accurately measure particle motion due to phase shifts within the first few octaves above the natural frequency. Even if these inaccuracies in the sensor could be eliminated or corrected for, the geophone suffers from high-frequency self-noise⁷ which reduces the potential signal-to-noise ratio above approximately 200 Hz.

8.1.2 Accelerometer-Based Seismic Receiver

The accelerometer-based Advanced Borehole Receiver, available from OYO Geospace Corp., Houston, TX⁷ was utilized as the seismic receiver for the suitability experiments. The receiver consists of two pressure housings fitted with standard Gearhart-Owens seven conductor cable-heads, one on either end of the clamping section. One housing contains the tri-axially arranged accelerometers. The orientation of the accelerometers are vertical, parallel to the clamp mechanism travel direction, and perpendicular to the clamp travel direction. The other housing contains the electric gear-motor assembly. This gear-motor drives the rectangular piston perpendicular to the longitudinal axis of the tool through the use of a 1:1 right angle gearbox to clamp the tool into the borehole.

Finite element analysis of the tool was previously performed to assure the clamping mechanism would maintain the potential for a flat tool response out to 2.0 kHz. The analysis resulted in a clamping piston design with 1.5 inches of travel, and accommodation of adapters to allow for clamping into boreholes ranging from 4.25 inches to 9 inches in diameter. The clamp force to tool weight ratio developed by this design is a function of the gearset selected to mate with the electric motor, and can vary from 5:1 to 20:1.

The low-noise piezo-electric accelerometers utilized in the receiver offer significant advantages over conventional geophones. In particular, these accelerometers do not exhibit the spurious resonance problem common to geophones. Additionally, accelerometers are insensitive to their mounting orientation and therefore do not require the gimbal mounts often utilized in geophone-based sondes. Another difference, and perhaps most important, is that these custom-designed low-noise piezo-electric accelerometers are more sensitive than geophones at the higher seismic frequencies. The high-frequency sensitivity improvement is due to the fact that the electronic noise of the custom accelerometer is lower than the electronic noise of the best geophones at frequencies above approximately 150 Hz. To illustrate this point, Figure 12 displays the seismic noise level in deep wells as compared to the noise limits of both geophones and accelerometers (the 2300 Hz accelerometer is the unit used in these experiments). It is apparent from Figure 12 that the accelerometers can offer as much as a 10:1 improvement in signal detection (and hence signal-to-noise ratio) at 1000 Hz. This signal-to-noise improvement has been demonstrated with this accelerometer receiver in numerous wells throughout the US. The specifications for these unique borehole accelerometers were developed by Sandia and resulted in a custom sensor which is now available from Wilcoxon Research as model 731-20.

8.1.3 Recommendations from the Suitability Test

In order to obtain optimal data, it is advantageous to use a seismic receiver that can detect the broadband emissions without the distortions caused by tool resonances. Normal wall-locking tools, such as those used for VSP surveys, are not capable of faithfully recording the particle motion over a wide frequency range. Advanced tools, using novel clamp designs and modal analysis to eliminate unwanted resonances, can provide the necessary detection capabilities. It is also important to take special precautions to assure that the receiver is adequately coupled to the borehole, irrespective of casing conditions. Special clamp procedures should be developed and tested.

Advanced accelerometer technology provides significant enhancements over geophones for detection of broadband emissions. Accelerometers should be considered for all microseismic mapping experiments where high frequency data are considered important. Additionally, due to the different types and strengths of microseismic signals, it is imperative to record continuously on wide-band-width, wide-dynamic-range recorders.

While polarization and P-S separation techniques can provide estimates of the locations event origin, difficulties in determining S-wave arrival points and vertical-plane polarization (inclination) make single station receiver technology less accurate in layered media. Future testing should be conducted with multi-station receivers. Additionally, accurate determination of the absolute orientation of the receiver(s) is imperative. While cross-well shooting can be used to determine a reasonably accurate tool orientation, a gyro or other means should be considered for an accurate, ground-truth orientation of the receiver(s).

Microseismic fracture mapping will only become a viable technology if techniques are developed to automate the processing as much as possible. Only a small fraction of the detectable microseisms can be processed individually by an analyst, at considerable time and effort. Such desirable processing capabilities include a real-time event detector, event-location processing, spectral analysis, event activity histograms, and classification of signal types.

8.2 M-Site Multi-Level and Treatment Well Diagnostic Test

Because of delays in funding, it was not possible to install the monitor well and begin fully instrumented experiments. However, there were several objectives that could be met using a single offset well and a treatment well, and an experiment was planned to obtain the needed information. This experiment was conducted in late October and early November of 1993.

8.2.1 Objectives

1. Monitor fracture geometry from an offset well using the greater accuracy derived from a multi-station receiver.
2. Compare a multi-station monitoring experiment with a single station experiment (i.e., the suitability test).
3. Compare the multi-station results with the treatment-well receiver data.
4. Use the diagnostic information on length and height to begin validating models.
5. Compare height from H/Z logging (Teledyne's technique) to that derived from microseisms (first time validation for this technique).

6. Compare the noise-polarization azimuth (Teledyne's technique) to the azimuth obtained from offset-well microseismic data (first time validation for this technique).
7. Test the data-acquisition systems for bugs and problems.
8. Determine instrument spacing requirements.
9. Obtain a full tomographic survey of the site for velocity structure.
10. Determine the effect of velocity structure on microseismic analysis errors.

8.2.2 Instrumentation Modifications

In order to run a multi-level fracture diagnostics experiment, several modifications were made to the receiver system. The data acquisition system was modified so that the data could be streamed directly to a Metrum VLDS recorder. This feature provides full back-up of all seismic energy detected by the multi-level receiver system.

To facilitate data processing, an event detector was added to the seismic digital field monitor (OYO DFM-480) in the multi-level wireline truck. This event detector, constructed in software, is set up to amplitude trigger on any combination of channels, at any desired amplitude. Amplitude settings can be changed at any time during a test as background noise levels change. The flexibility in triggering channels allows the operator to eliminate any noisy channels that might trigger inappropriately.

The seismic digital field monitor was also interfaced to the CER M-Site network, and the event detector software modified to write event files to the network, as well as to its own hard disk. The capability allowed events to be sent directly to processing and analysis stations.

Rails were added to the back side of the receiver (opposite the clamp shoe) to enhance stability of the receivers and improve fidelity of the signals recorded. This feature further minimized any tool resonances and instabilities.

To conduct an H/Z survey with orientation, an analog receiver (run on 7-conductor wireline) was modified to accept interfacing with a GyroData orientation tool. This was done using an electronic switch to allow operation of the GyroData tool when the accelerometers were powered off.

8.2.3 Test Plan

The test plan for the 1993 M-Site multi-level and treatment well test consisted of two parts: a detailed velocity survey and a series of monitored fracture experiments. The velocity survey was conducted during the last week of October, 1993, and the fracture experiments were conducted during the week of November 1, 1993. Both of these tests used the Sandia/OYO multi-level, accelerometer-based receiver string, run by Bolt on a Chevron fiber-optics wireline.

Specific activities included:

WEEK 1: SET UP, VELOCITY SURVEY AND ORIENTATION

OCT 25, 1993	SET UP FOR TOMOGRAPHIC SURVEY
OCT 26, 1993	CONTINUED SET UP; FIRST SURVEY SCANS
OCT 27, 1993	SURVEY
OCT 28, 1993	FINISH SURVEY SET UP FOR FRAC
OCT 29, 1993	ORIENTATION (TEST SHOTS + SCAN)

WEEK 2: FRACTURE EXPERIMENTS

NOV 1, 1993	FRAC # 1	BHP GAGE IN FRAC WELL MULTI-LEVEL RECEIVERS IN OFFSET WELL
NOV 2, 1993	FRAC # 2	NO BHP GAGE SINGLE RECEIVER + GYRO IN FRAC WELL MULTI-LEVEL RECEIVERS IN OFFSET WELL
NOV 3, 1993	RESOLVE INSTRUMENTATION & WIRELINE PROBLEMS	
NOV 4, 1993	FRAC # 3	NO BHP GAGE SINGLE RECEIVER IN FRAC WELL MULTI-LEVEL RECEIVERS IN OFFSET WELL
	FRAC # 4	NO BHP GAGE; STATIC COLUMN IN FRAC WELL GAMMA TOOL IN TUBING OF FRAC WELL MULTI-LEVEL RECEIVERS IN OFFSET WELL

8.2.4 Tomographic survey

The tomographic survey was conducted using the multi-level system, with 5 separate receivers spaced at 10 ft intervals. The receivers were located in well MWX-2 and a Bolt airgun, used as the source for the survey, was run in MWX-3. The range of shot and receiver locations is shown schematically in Figure 13. Receivers were moved at 10 ft increments between 4500 ft and 5000 ft, while airgun shots were positioned at 5 ft intervals between 4500 ft and 5200 ft. Fill-in receiver data at 5 ft intervals were then conducted between 4800 and 5000 ft.

This tomographic survey used the 5-level receiver system with a moving airgun source to obtain an incredible amount of data in a short time. The amount of data and the times are given below:

date	<u>shot-receiver scan</u>	<u>time</u>
10/26	750	2 hr
10/27	6750	8 hr
10/28	<u>2100</u>	<u>3 hr</u>
total	9600	13 hr

In fact, since these tests were conducted over a three day period, there are three separate set-up periods and the actual data-acquisition time is closer to 10 hr. Using standard industry equipment and procedures, 9600 scans would typically take close to a week to complete.

The data from the tomographic survey are high quality, with clear p-wave arrivals. Figure 14 shows a vertical-component common receiver gather of raw data for a receiver at 4820 ft and airgun depths from 4500 to 5200 ft (141 traces). Generally, there are good signal-to-noise ratios for these traces with excellent P-wave first-arrival standout and visible S waves. There are some receiver resonances around 1500-2000 Hz (accelerometer resonances) and what appears to be airgun resonance at 550 Hz. There is also a sharp spectrum rolloff above 550 Hz, which is typical behavior for the airgun source.

Figure 15 shows the same data after bandpass filtering with a 300 Hz high cut filter. This filter removes the resonance effects, yielding a much improved signal-to-noise ratio, particularly for the S-waves (which are lower frequency than the P-waves). There are lower amplitude P and S first arrivals on the vertical component when the airgun is close to the receiver depth. This behavior is expected due to the strong radial directionality of the source P-wave radiation pattern. It is also possible to see the polarity reversals in both P and S(S_V) arrivals as the airgun scans past 4820 ft depth and the direction of the first motion changes. Finally, both up- and down-going tube waves are clearly visible.

The analysis of the velocity survey will be completed during 1994. These results will be used to improve microseismic interpretation schemes and develop error estimates.

8.2.5 Orientation of Receivers for Fracture Experiments

After completing the velocity survey using a 5-level receiver system, the receivers were pulled out of MWX-2 and reconfigured for the fracturing experiments. To obtain the widest possible receiver aperture, it was necessary to reduce the system to 4 levels, with a 10 ft interconnects between the top three receivers and a single 50 ft interconnect between the third and fourth receiver. The receivers were then positioned at 4885, 4895, 4905 and 4955 ft in MWX-2 (the offset well).

The receivers were oriented by first conducting 7 test air-gun shots at 4700 ft, and then conducting a full air-gun scan from 4700 to 5150 ft at 10 ft intervals. The polarization plots from one of the air-gun scan shots, using unfiltered data, are shown in Figures 16 through 19. Figure 16 gives the important data of the top-level receiver (at 4885 ft) for a shot at 4930 ft depth in MWX-3. At the bottom are the three components, at the top left is the horizontal polarization, and at the top right is the vertical plane polarization. Data associated with the shot, polarization, etc. are given on the far right. For this particular shot and level, the horizontal polarization is very tight, but the inclination is questionable. Many of the test shots had inclination polarizations that were difficult to interpret, presumably because of the layering.

The horizontal polarization data from Figures 16-19 show that the receivers have rotated considerably relative to each other, with relative orientations of 0.5°, -74°, 88.3°, and 85.2°. Using a large number of the scan shots, it is possible to obtain statistically accurate orientations for the receivers. Figure 20 and Table 1 show the relative orientations at each of the four receiver levels for shots between 4800 and 5010 ft. The data are clearly consistent, with small standard deviations.

8.2.6 Fracture Experiment # 1

The first fracture experiment was designed to be a test of the diagnostic capabilities of a multi-level system. For direct comparison with the fracture models, a bottom-hole pressure gage was run in the treatment well. The injection consisted of 450 bbls of a 40# linear gel, pumped at a rate of 25 bpm. Two shut-ins were also conducted during the first half of the treatment.

During this first injection, the multi-level system detected 89 discrete events, of which 77 were analyzable microseisms. Figures 21-24 show example data from one of microseisms as detected on each of the four levels. This particular microseism is slightly to the east of the treatment well, as can be seen by comparing the relative azimuths of the microseisms to the relative azimuths of the orientations shots, as given in Figure 20. In many of the recorded microseisms, both the p-wave and the s-wave can be easily distinguished. However, some of the microseisms have s-wave arrivals that are difficult to pick. Criteria for accepting an s-wave arrival include:

1. change of polarization (90°)
2. change of frequency (decrease)
3. change of amplitude

However, there are a number of microseisms in which all three of these criteria can not be met.

A preliminary map of the fracture is shown in Figure 25. This figure is derived from unfiltered data without any incorporation of velocity structure. Because of the significant layering in the formation, it is quite likely that the horizontal position of the mapped points could be considerably in error, but these questions will be resolved when the velocity structure is considered. On the other hand, the length of the fracture is not likely to change significantly because the inclination angle is relatively small (typically less than 20°). The top left graph in Figure 25 shows a plan view which depicts an asymmetric fracture with wing lengths of about 120 ft and 250 ft. The wells are shown as squares and a regression line through the microseisms gives an azimuth of $N70^\circ W$. The top right graph shows a side view projection normal to the fracture azimuth (as determined by the regression), the location of the treatment well, and a projection of the receiver string, all relative to the gross sand thickness. Most of the growth appears to be upward, but this possibility will not be confirmed until all information is considered (e.g., data filtering, velocity structure). The bottom graph shows the time at which events were determined relative to the pressure at that time. Some events were probably missed at the beginning of the treatment because trigger levels were high, but these events are all likely to be near the wellbore and they can be obtained by playback of the raw data from the Metrum VLDS recorder.

8.2.7 Fracture Experiment # 2

The second fracture experiment was also run with a four-level system in the offset well, but a single seismic receiver was also run in the treatment well. The injection consisted of 400 bbls of 40# linear gel, pumped at 15 bpm, with three shut-in throughout the treatment.

The single seismic receiver was interfaced with a GyroData tool for orientation, run down below the perforations, and clamped in place. During the injection, this receiver was monitoring for microseisms that could be detected from the treatment well. In order to correlate with microseisms seen by the multi-level system, IRIG-B signals were used for timing.

After the treatment, an H/Z logging run was performed, with data being taken at 50 ft stations for four-minute intervals. Data were recorded continuously on a SONY DAT recorder at 12 kHz. The following table gives the H/Z stations and the orientation of the receiver from the GyroData tool.

Depth (ft) in MWX-3	Orientation
5300	359
5250	274
5200	293
5150	327
5100	68
5050	91
5000	105
perfs	
4850	65
4800	72
4750	61
4700	60
4650	80
4600	76
4550	356
4500	89

These data have not yet been analyzed, pending the completion of additional software for using the GRI H/Z analysis system.

Treatment well microseisms have not yet been examined, pending final resolution of velocity structure. It was noted, however, that the GyroData tool adds a significant resonance to the tool at about 400 Hz.

The multi-level system recorded 161 events which are now being analyzed. These events look very similar to those seen in the first fracture experiment.

8.2.8 Fracture experiment # 3

Fracture experiment # 3 was a repeat of the second fracture experiment, except that there was no GyroData tool on the single seismic receiver. This test was intended to obtain the best possible H/Z data and treatment well microseismic data. H/Z station were located at 50 ft intervals from 5300 up to 4500, with the station at 4900 ft moved to 4895 to avoid perforations.

Data from this test have not yet been analyzed. The multi-level system recorded 129 events.

8.2.9. Fracture experiment # 4

The fourth fracture experiment was a sand injection using 484 bbls of 40# linear gel, 144 bbls of 40# cross-linked gel, and 16,400 lbs of sand, pumped at about 15 bpm. The multi-level system recorded over 100 events that have not yet been analyzed.

8.3 Monitor Well Design

The focus of activities at M-Site during 1993 and 1994 will be on validating diagnostic techniques and models. In order to perform an acceptable validation, it is necessary to establish some baseline ground truth. The M-site experiment ground truth will be established through the use of a highly instrumented monitor well, which will include both seismic instruments and downhole tiltmeters (which will be referred to as inclinometers).

Preliminary plans call for 30-32 tri-axial seismic levels at 30 ft spacing and 6 biaxial inclinometer levels at 50 ft spacing through the two zones of interest.

8.3.1 Seismic instrumentation

Accelerometers have been chosen for the seismic transducers in the monitor well. Even though accelerometers are more expensive than geophones, their noise-floor and frequency-response characteristics make them especially well suited for this experiment (see section 8.1.1 and 8.1.2). The Wilcoxon Research Model 731-20 Seismic accelerometers are an example of an acceptable instruments; their characteristics are:

Sensitivity	20 Volts/g
Amplitude range	0.2 g peak
Amplitude nonlinearity	1%
Frequency response	±3 dB from 1.5-1200 Hz
Resonance frequency	>2200 Hz
Transverse sensitivity	<4% of axial
Electrical noise	<1 µg broadband (2 Hz - 20 kHz) -158 dB re g/√Hz at 100 Hz -163 dB re g/√Hz at 1000 Hz
Temperature range	-40 - 120° C
Vibration limit	50 g peak
Shock limit	200 g peak

The second major requirement for the seismic instrumentation is a complete data acquisition system. With as many as 32 levels, and each level containing three channels, a high-speed 96 channel data acquisition system (DAS) is required. We have found such a system in the OYO Geospace DAS-1. Particularly impressive is the 24 bits of resolution at which the system can digitize. Some modifications of the system would be required, and these will be considered in 1994.

8.3.2 Inclinometers

The inclinometers chosen for this application are Applied Geomechanics Model 510 Geodetic Borehole tiltmeters. These gages have the following characteristics:

Resolution	10 nanoradians
Operating tilt range	±900 µradians
Leveling range	±3°
Temperature	70°C
Pressure	>3000 psi (tested at Sandia)

These tiltmeters appear ideal for both small inclinations that are expected during stress tests and large inclinations during fracture treatments.

8.3.3 Cabling

Data telemetry of all these gages will be handled with two separate cables. Defining details of the cable design is an ongoing task.

9.0 Other Diagnostic Tasks

9.1 H/Z Analyses

Sandia is working on implementing the H/Z analysis for GRI sponsored research. All of Teledyne Geotech's tape data are now at Sandia and the source files for the H/Z work have been obtained. Sandia has begun the procurement process for getting Jim Fix on as a consultant to assist in H/Z analysis.

9.2 Industrial Partner for Seismic-Based Diagnostics

GRI and Sandia have begun the process for obtaining an industrial partner to market diagnostic technology developed under this contract.

10.0 REFERENCES

1. Warpinski, N.R., Teufel, L.W., Lorenz, J.C. and Holcomb, D.J., "Core Based Stress Measurements: A Guide to Their Application," GRI-93/0270, June 1993.
2. Warpinski, N.R., Abou-Sayed, I.S., Moschovidis, Z. and Parker, C., "Hydraulic Fracture Model Comparison Study: Complete Results," GRI-93/0109, February 1993.
3. M-Site Project Group, "Multi-Site Project Seismic Verification Experiment and Assessment of Site Suitability," GRI-93/0050, February 1993.
4. Sleaf, G.E., Warpinski, N.R. and Engler, B.P., "The Use of Broadband Microseisms for Hydraulic Fracture Mapping," SPE 26485, Proceedings, 68th SPE Annual Tech. Conf., Houston, TX, Vol. 2, pp. 707-717, Oct. 3-6, 1993.
5. Gaiser, J.E., Terrance, J.F., Petermann, S.G., and Kemer, G.M., "Vertical Seismic Profile Sonde Coupling," *Geophysics*, Volume 53, Pages 206-214, Feb., 1988.
6. Stanley, P.J., "The geophone and front-end fidelity," *First Break*, Vol. 4, No. 12, pp. 11-14, 1986.
7. Sleaf, G.E. and Engler, B.P., "Experimental Study of an Advanced Three-Component Borehole Seismic Receiver," Proceedings, 61st Annual SEG Meeting, Houston, TX, pp. 30-33, 1991.

11.0 MAJOR ACHIEVEMENTS

Major achievements include:

Completion of the topical report on core-based stress measurements and the associated CER/Sandia topical report on methods for determining stress azimuth

Completion of work on the Frontier outcrops and the preparation of a topical report on those studies. These outcrop studies provide the basis for an explanation of the fracture systems that should be expected in the Frontier formation within the Moxa Arch area.

Completion of a topical report detailing all of the results of the Hydraulic Fracture Propagation Modeling forum.

Completion of the M-Site suitability test analyses and the preparation of a topical report, a SPE paper, and an SEG abstract/presentation detailing those results.

Design, testing, and initial analysis of multi-level diagnostic experiment in the A sand at M-Site. In the four fracture treatments conducted during this test, an event detector was used to identify microseisms and write them to the network for operator analysis, proving the concept that will be employed during full-scale M-Site testing.

Identification of accelerometers, tiltmeters, data acquisition, and full-backup recording equipment to be used for the new M-Site monitor well.

12.0 MAJOR PROBLEMS

No major problems were encountered during 1993.

13.0 CONCLUSIONS

Results of core-based stress measurements, when compared with other core data, have been found to be reliable indicators of stress azimuth (and in some cases magnitude), but it is necessary to have good quality control and critical examination of the data and to perform auxiliary measurements in some cases to ascertain the accuracy and reliability of the measurements. The application of these measurement techniques is described in detail in a just-completed topical report.

Natural fractures are an important element of production from tight rocks in the Moxa Arch region of the Green River basin. However core and outcrop data have seemed to yield inconsistent numbers and orientations of fracture sets, particularly within the Frontier formation. A synthesis of outcrop data from along the Oyster ridge hogback on the western edge of the Green River basin has now yielded a clearer picture of the fractures and their relationship to tectonics and diagenesis. These results can be extrapolated into the basin to provide a rationale for production from natural fractures. These results have been described in two topical reports that have been prepared and will be published in 1994.

The M-Site suitability test has been extremely important for identifying the characteristics of microseisms that must be faithfully recorded in order to obtain accurate mapping information. Details of the detection and recording requirements are described in an SPE paper. In essence, broadband seismic instrumentation (100-1500 Hz) are necessary if microseisms are to be adequately monitored.

The multi-level fracture experiment in the A sand at M-Site was successfully completed. Although data will continue to be analyzed for the next several months, the results of these tests show the importance of using multi-level systems if accurate microseismic mapping is to be performed. The fractures created during these tests are asymmetric both in length and height.

14.0 OBJECTIVES AND WORK PLANNED FOR NEXT YEAR

The work effort for next year will change focus because of an amendment to the contract which went into effect in October, 1993. Fracture diagnostics will comprise the bulk of the work activities that will be performed. However, some activities in stress, fractures and stimulation will continue.

In the area of in situ stress, some additional core-based stress measurements will be obtained to support M-Site and other GRI projects.

The topical reports on natural fractures in the Green River basin will be completed and published in 1994. Some additional core and outcrop studies will be performed in order to finalize the model of the fracture system as it exists at depth in the basin.

In the diagnostic area, analysis of the 1993 M-Site multi-level experiment will be completed and the resulting information will be used to plan processing schemes for microseismic data analysis and for the analysis of other types of seismic energy (e.g., fracture waves). Analysis of microseisms will include evaluation of raw data, as recorded directly by the event detector, of various forms of filtered data, of different location schemes, of the effects of layering, of the differences in treatment vs offset well data, of the differences in location within the treatment well, and other appropriate procedures. Other analyses include H/Z studies, a search of fracture waves, an examination of the range of seismic data, noise polarization, and others.

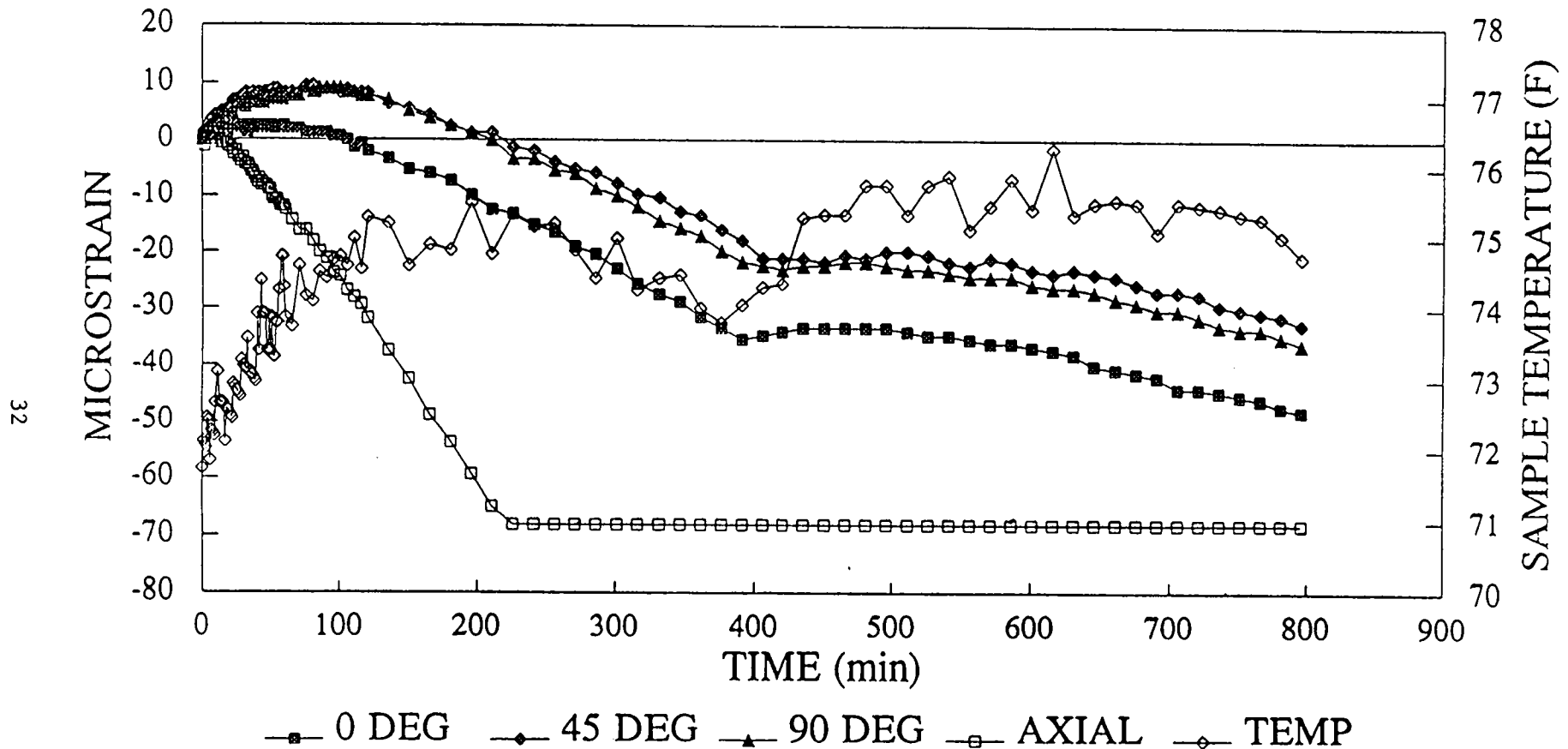
Design, fielding, and installation of the instrumentation for the M-Site monitor well will be completed in 1994. The major thrust will be on the cabling and data acquisition systems for the monitor well.

In 1994, a second M-Site experiment will be conducted in the B sand, at a depth of approximately 4500 ft. Expected tests are a three-well velocity survey, a series of monitored stress tests, and two fracture experiments. These tests will use instrumentation in the new monitor well, an offset well, and the treatment well. These combinations of monitoring locations should provide ground truth fracture data as well as the associated wireline data that will eventually be used as a gas-industry service.

Table 1
ORIENTATION SCAN AZIMUTHS
1993 M-SITE TEST

	LEVEL 1 (TOP)	LEVEL 2	LEVEL 3	LEVEL 4
4800	0.9	-63.8	81.1	78.7
4810	4.0	-78.6	82.3	77.2
4820	1.1	-72.5	81.2	76.2
4830	-3.6	-70.0	75.3	79.6
4840	-2.8	-66.1	78.5	79.6
4850	-1.2	-67.5	79.0	91.3
4860	-2.1	-67.2	88.7	86.5
4870	-4.5	-65.8	80.4	82.1
4880	-2.5	-68.1	86.9	79.6
4890	4.4	-66.5	88.9	84.4
4900	-5.2	-68.7	88.3	81.9
4910	-0.9	-72.4	83.8	83.4
4920	-5.0	-69.3	82.4	84.1
4930	0.5	-74.0	88.3	85.2
4940	-1.0	-70.3	87.8	86.7
4950	0.7	-68.8	90.7	84.2
4960	0.9	-69.8	94.5	80.8
4970	2.2	-68.3	89.0	85.6
4980	2.5	-69.1	89.2	81.3
4990	5.7	-67.5	91.3	84.8
5000	1.3	-65.9	93.2	84.0
5010	10.3	-64.7	95.4	84.1
AVG	-0.2	-68.9	86.2	82.8
ST DEV	3.1	3.3	5.5	3.5

ANELASTIC STRAIN RECOVERY



OCTOBER 9, 1993

SAMPLE #1 FILE ASRRWL1.WK3

Figure 1. Field data from sample #1, Amoco well.

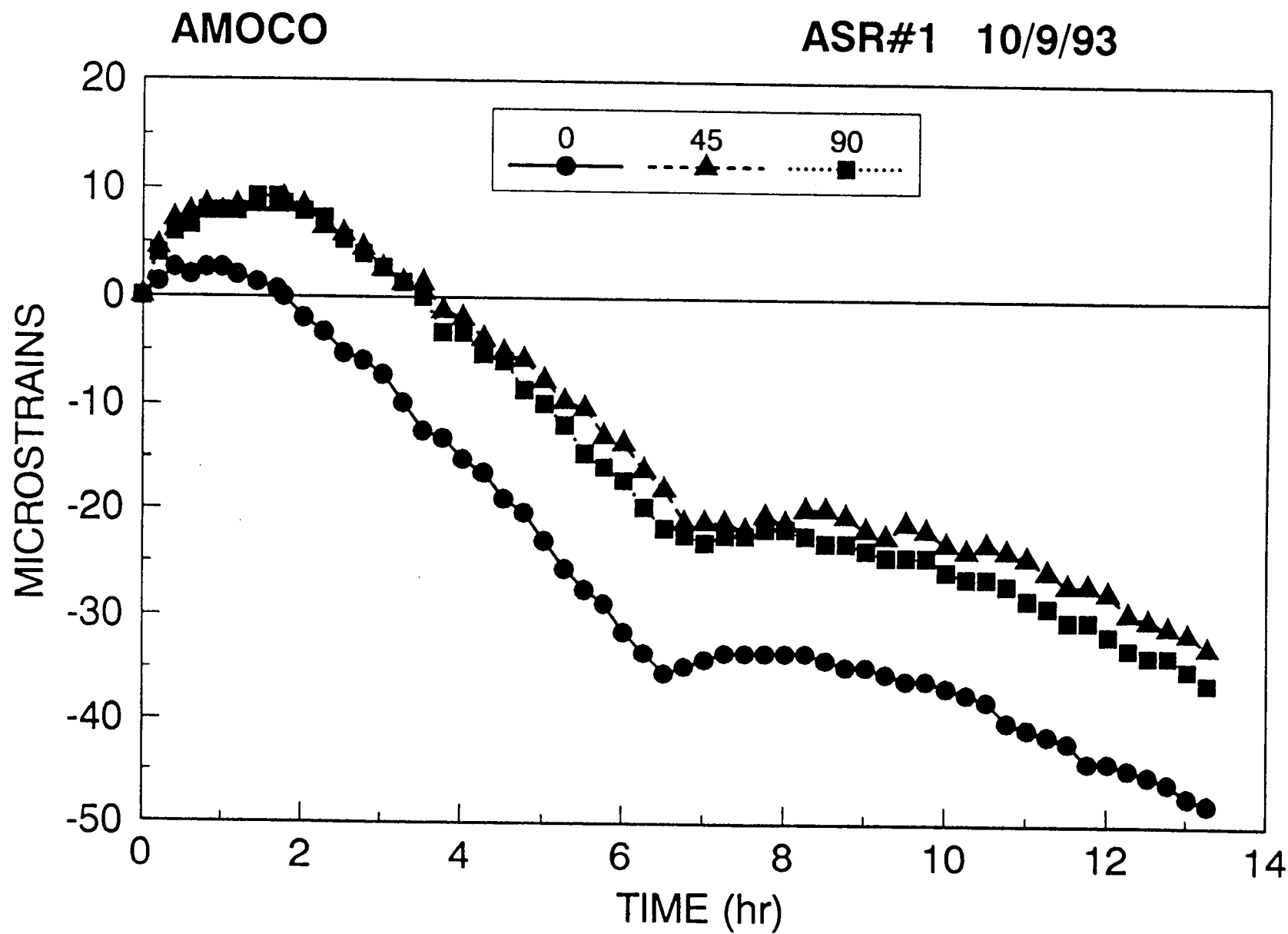


Figure 2. Usable horizontal strain data from sample #1, Amoco well.

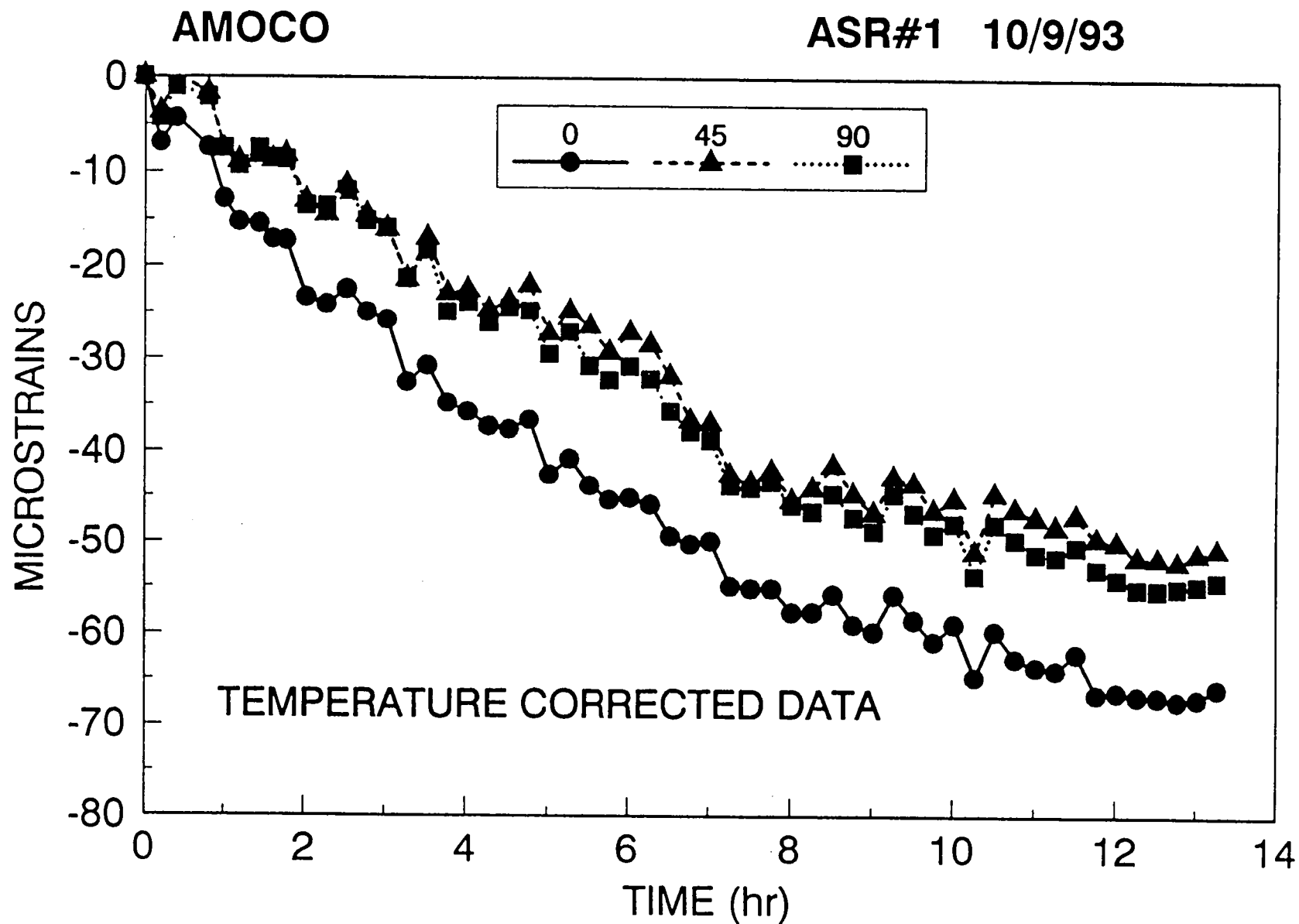


Figure 3. Corrected horizontal strain data from sample #1, Amoco well.

AMOCO

ASR#1 10/9/93

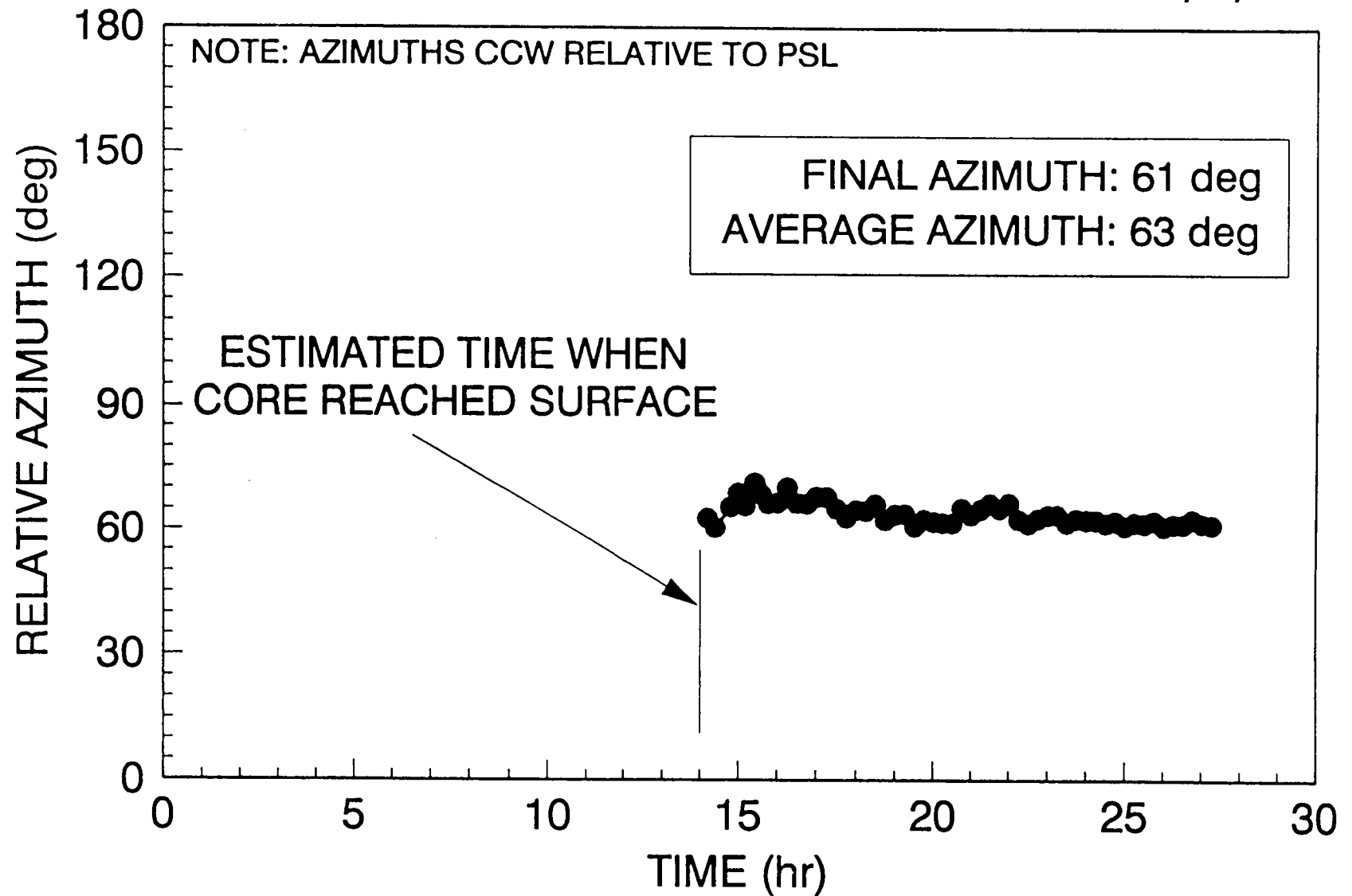
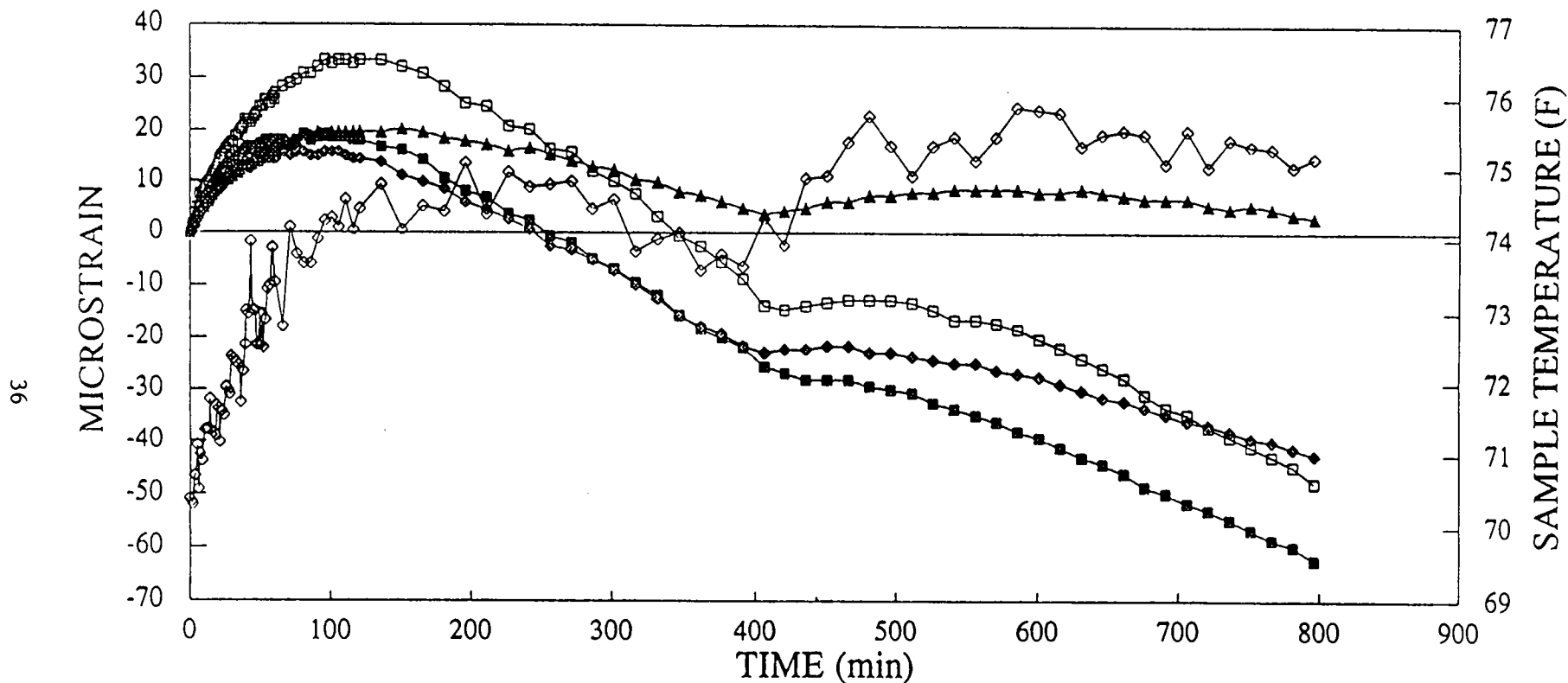


Figure 4. Relative azimuth results from sample #1, Amoco well.

ANELASTIC STRAIN RECOVERY



OCTOBER 9, 1993
SAMPLE #3 FILE ASRRWL3.WK3

Figure 5. Field data from sample #3, Amoco well.

AMOCO

ASR#3 10/9/93

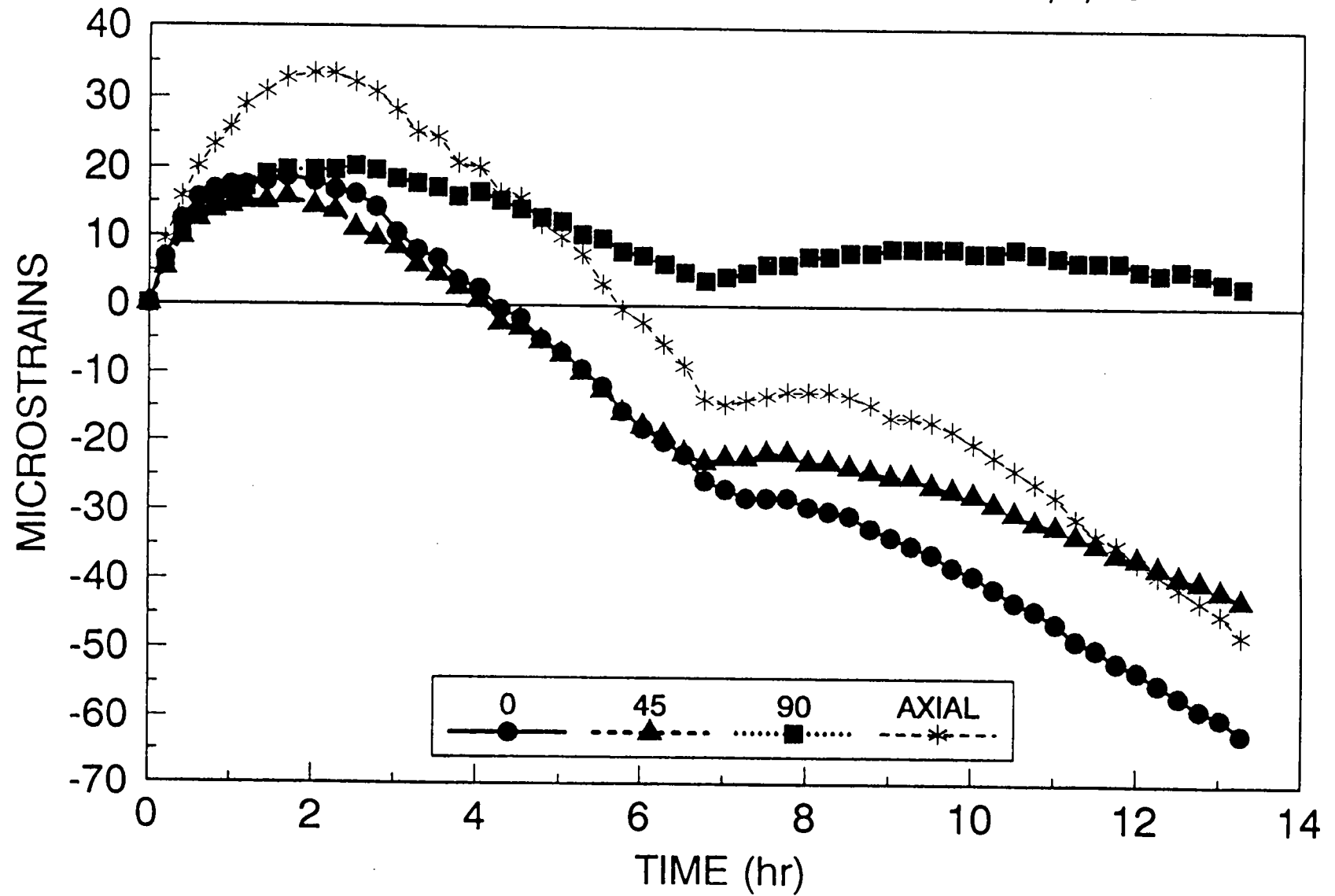


Figure 6. Usable strain data from sample #3, Amoco well.

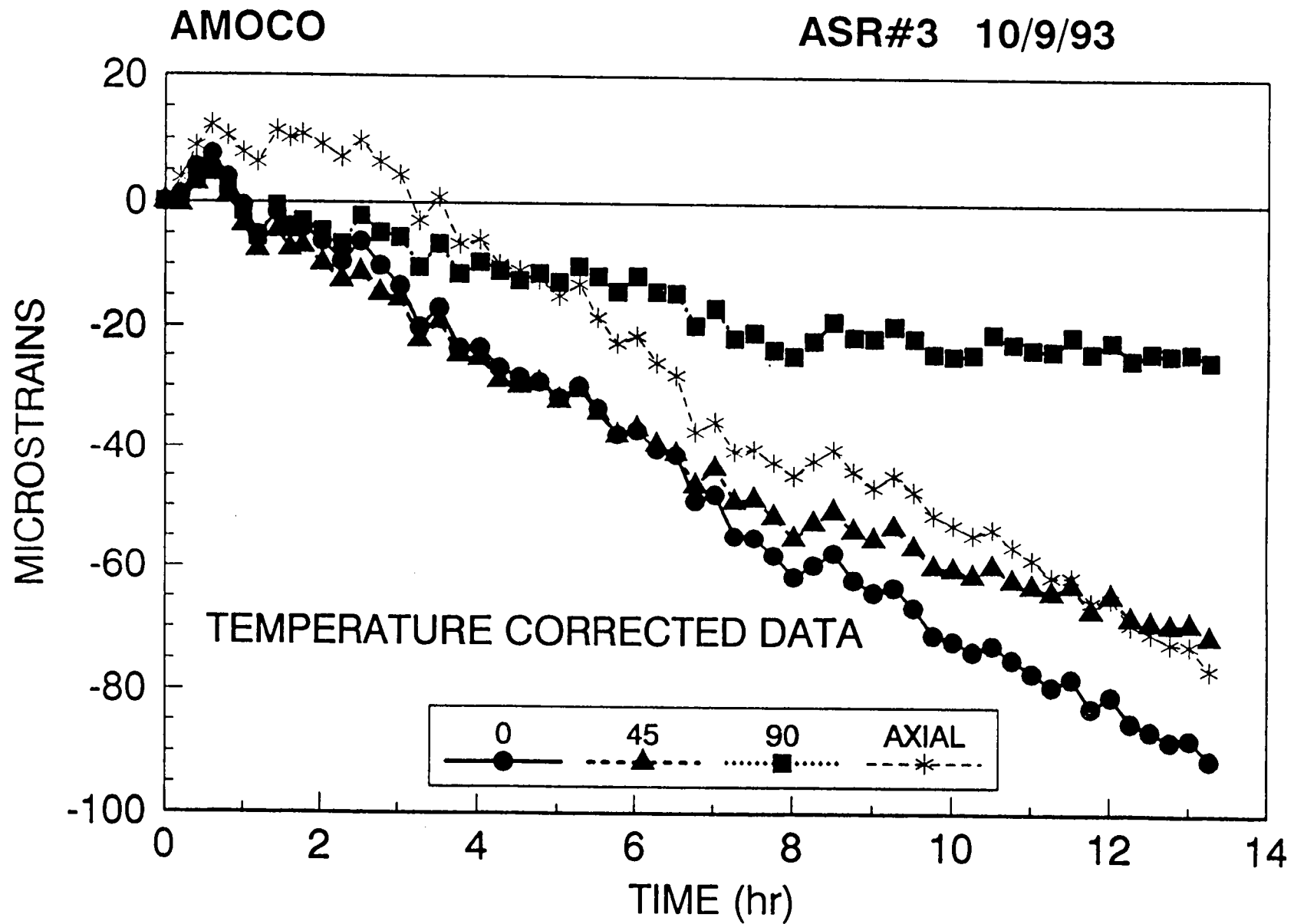


Figure 7. Corrected horizontal strain data from sample #3, Amoco well.



Figure 8. North-south striking J1 fractures

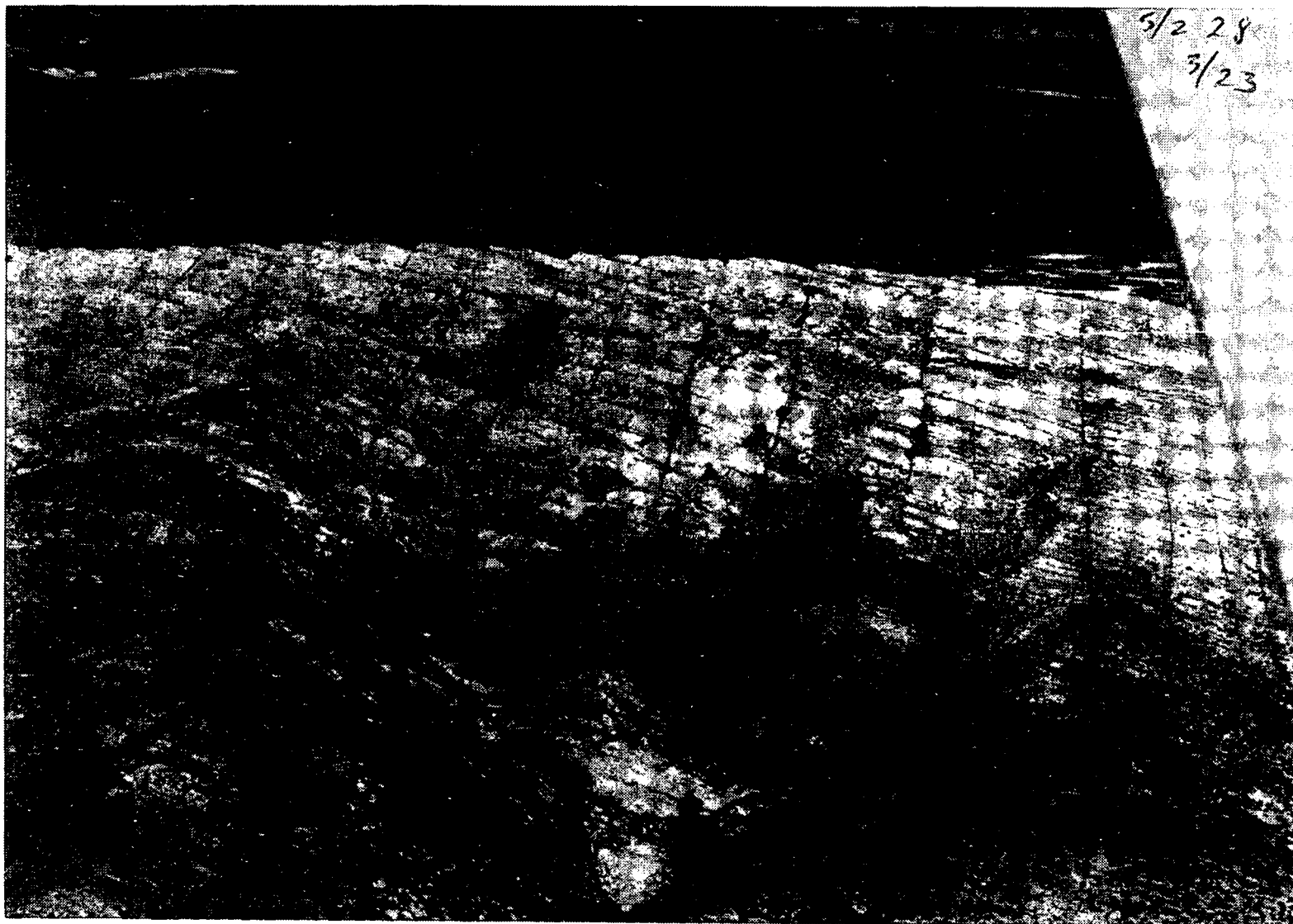


Figure 9. East-west striking J2 fractures superimposed on J1 fractures

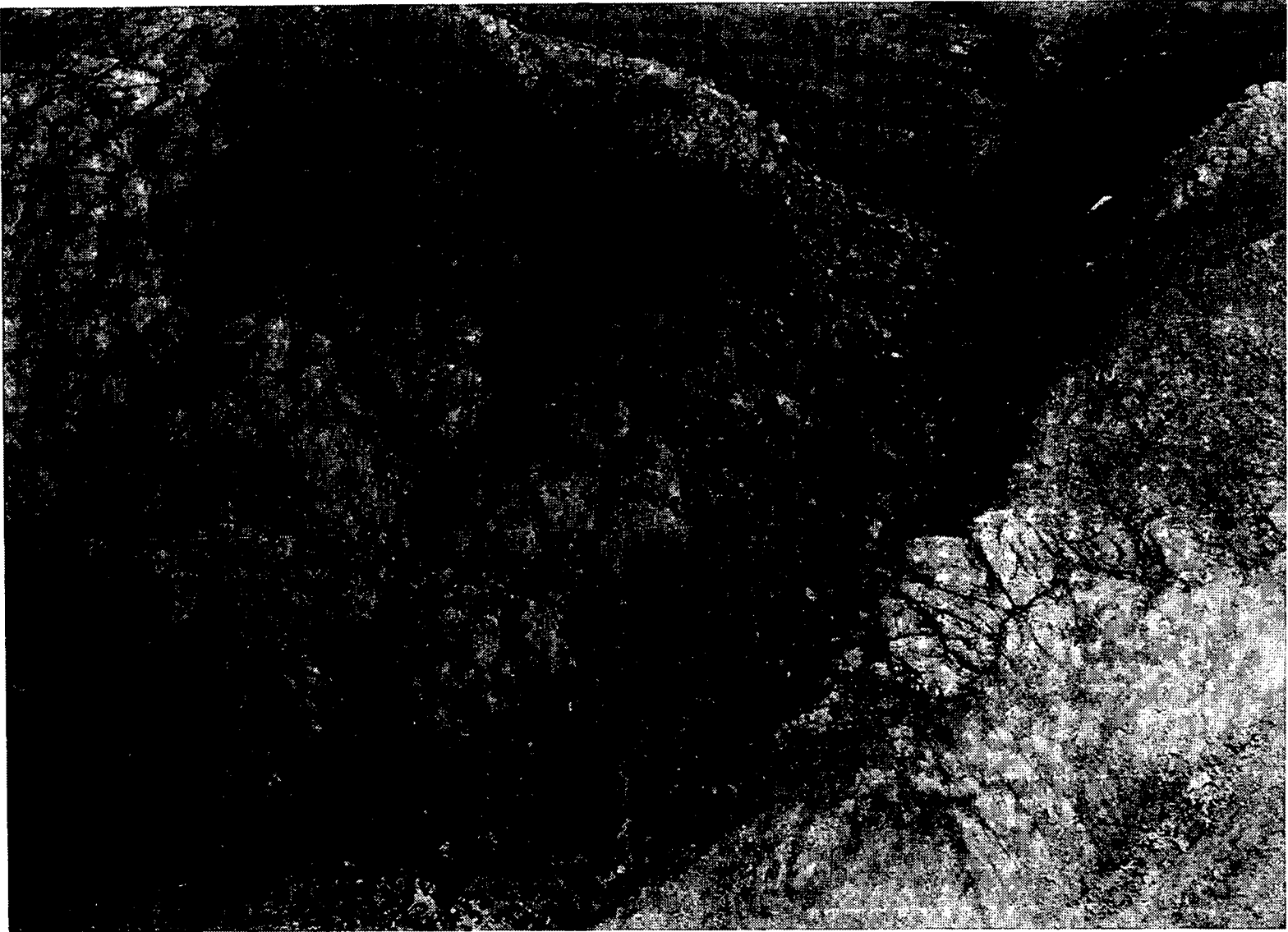


Figure 10. Irregular J3 fractures at a structural discontinuity along the thrust plate that forms the Hogsback

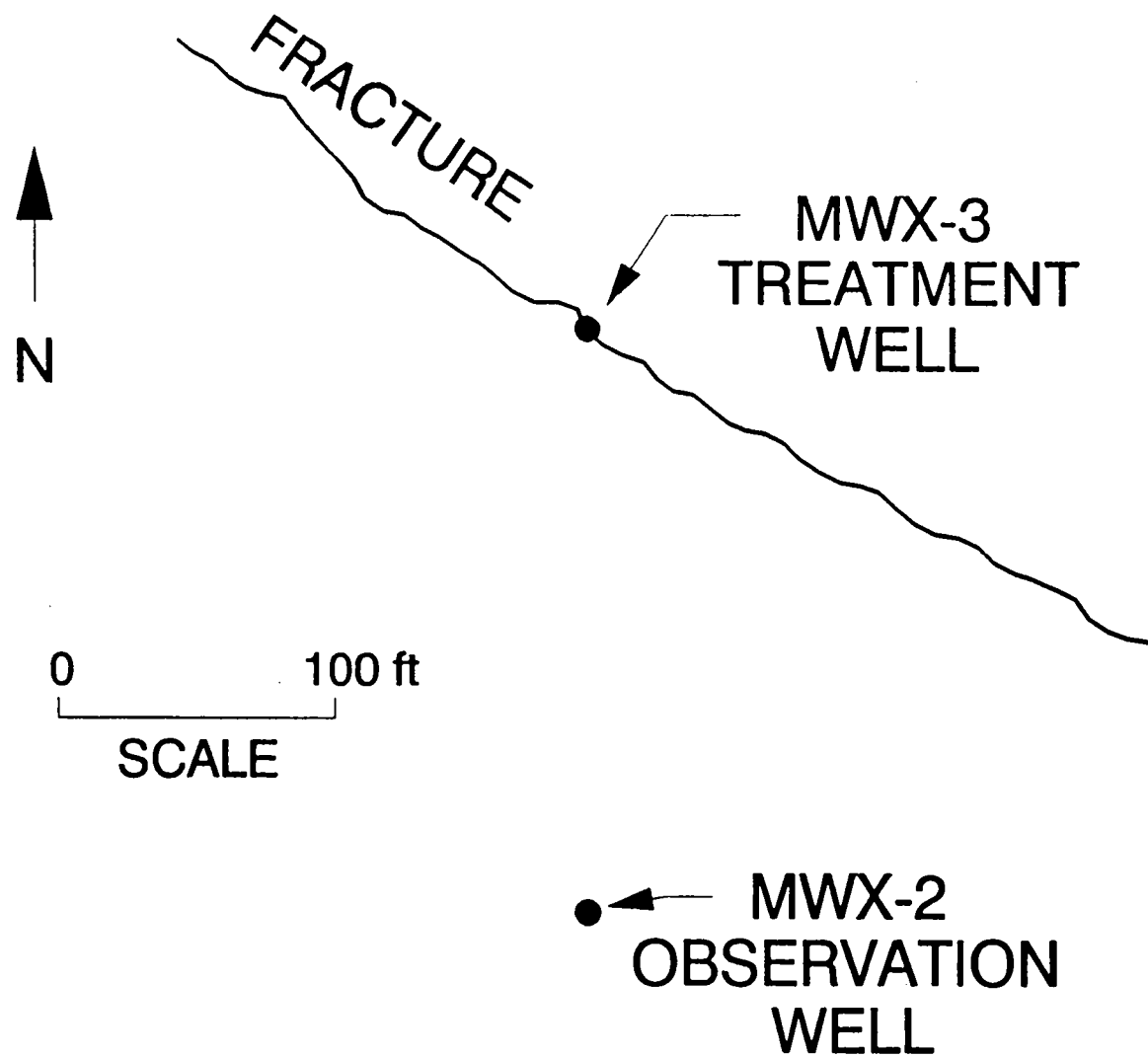
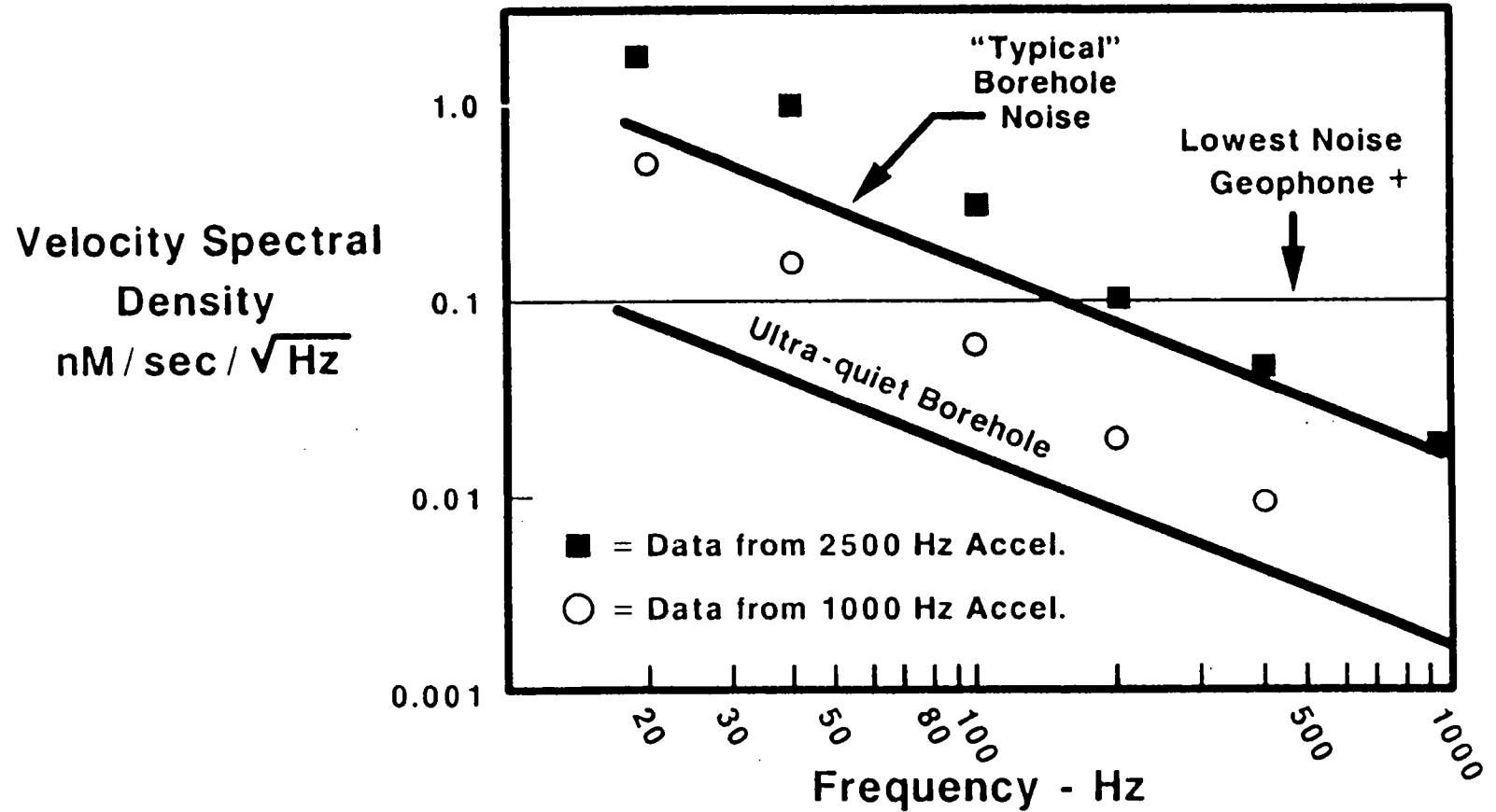


Figure 11. Current layout of M-Site experiment

Sensor Noise Limits ($T < 125^{\circ}\text{C}$)



+ 0.5 V/cm/sec., 1 K Ω Geophone with OPA37HT High-temperature amplifier

Figure 12. Noise limits of borehole seismic sensors.

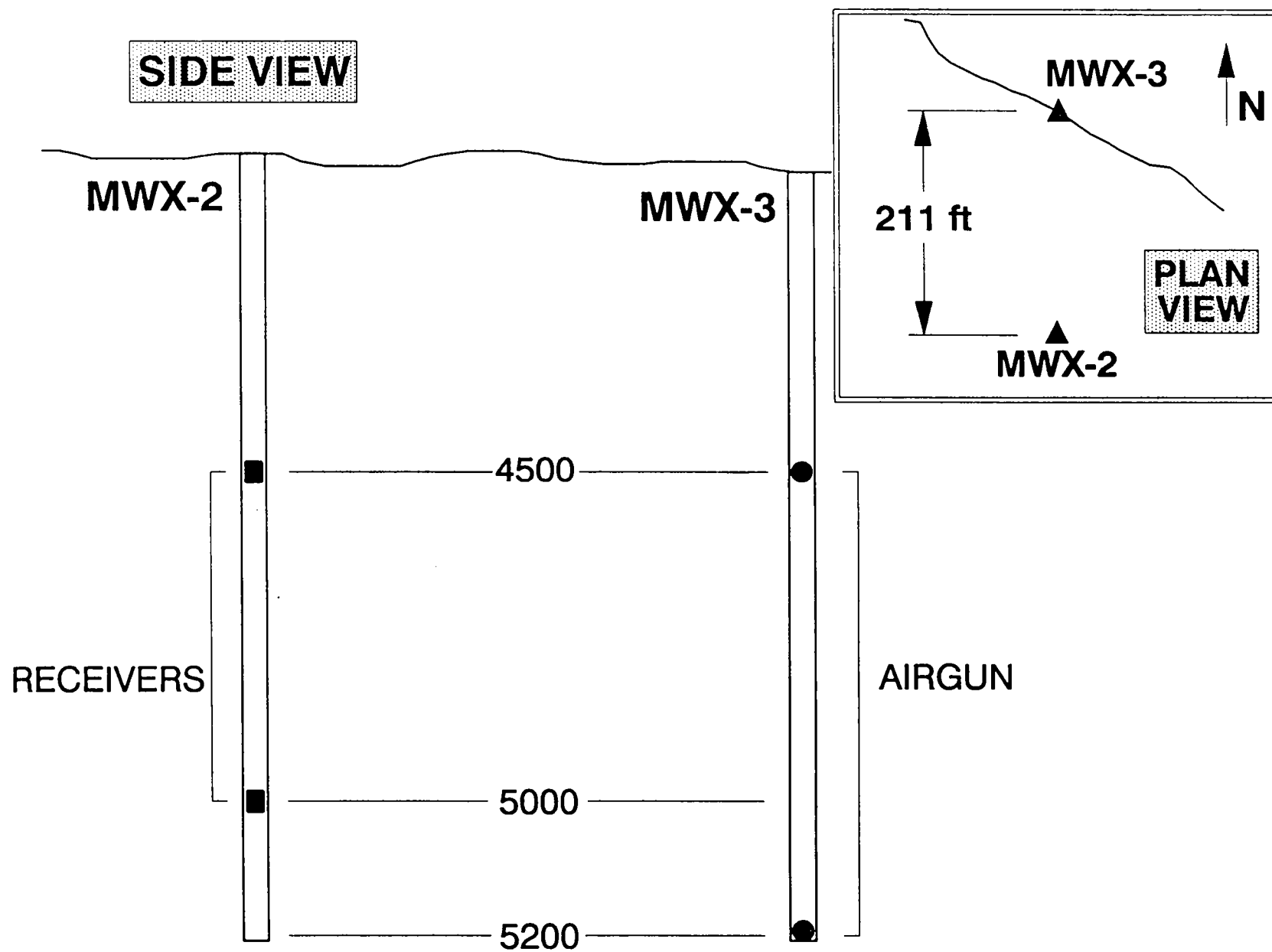


Figure 13. Schematic layout of crosswell velocity survey.

MULTIWELL CROSSWELL SEISMIC RAW DATA (Vertical Component)
Receiver at 4820'

Airgun Depth

4500' ⇒

4850' ⇒

5200' ⇒

0

.100

.200

Time/Sec

45

Figure 14. Common receiver gather of raw signals.

MULTIWELL CROSSWELL SEISMIC FILTERED DATA (Vertical Component)
Receiver at 4820'

Airgun Depth

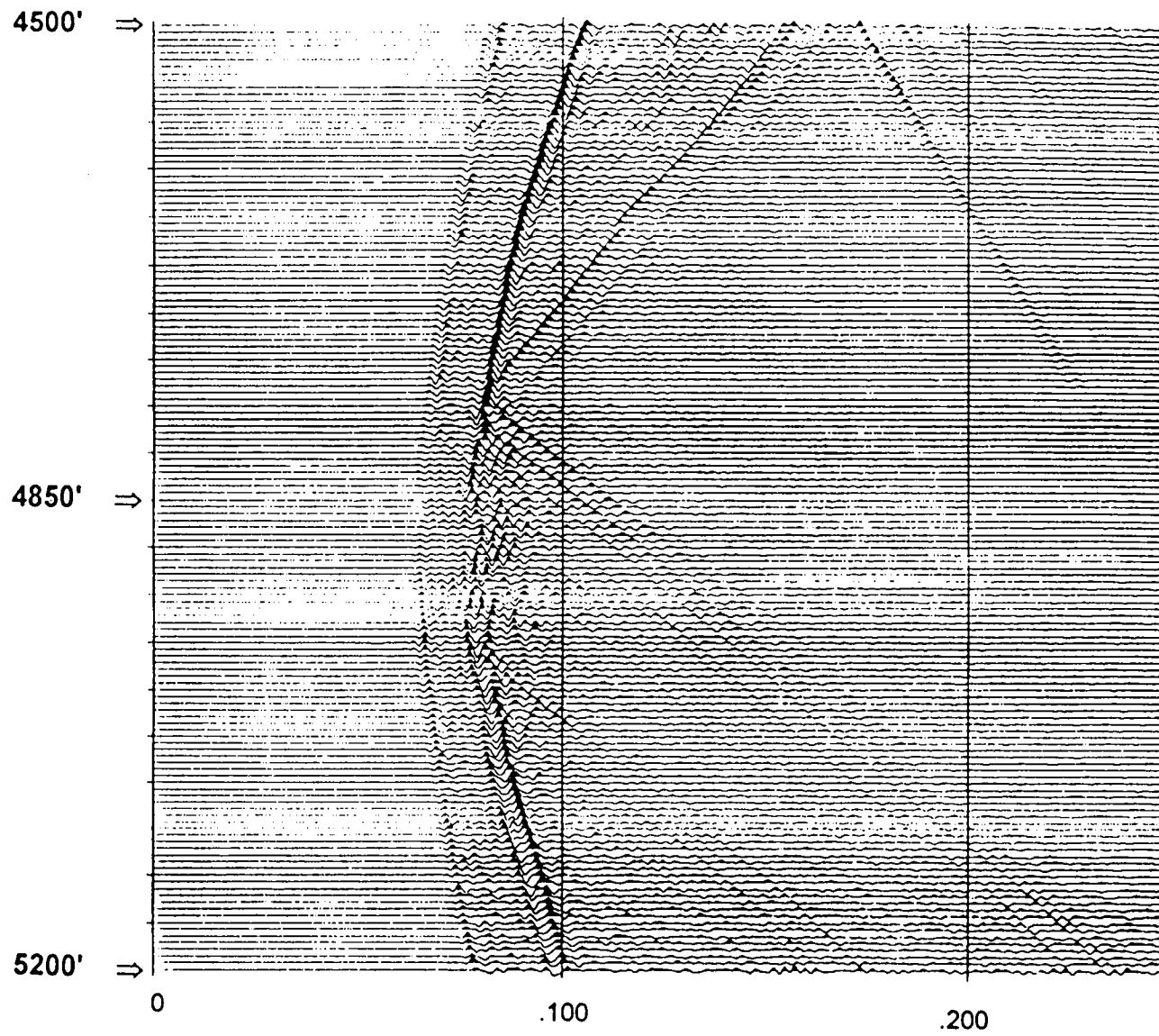
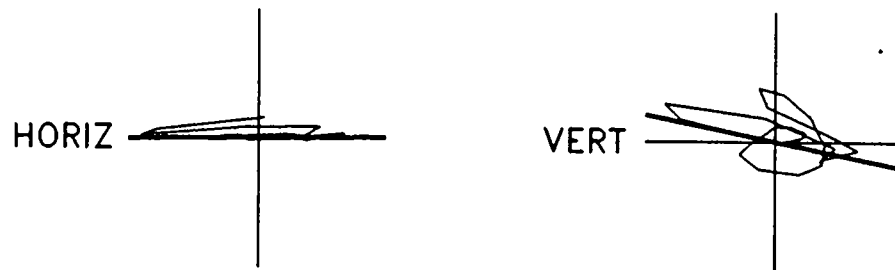


Figure 15. Common receiver gather of filtered data.

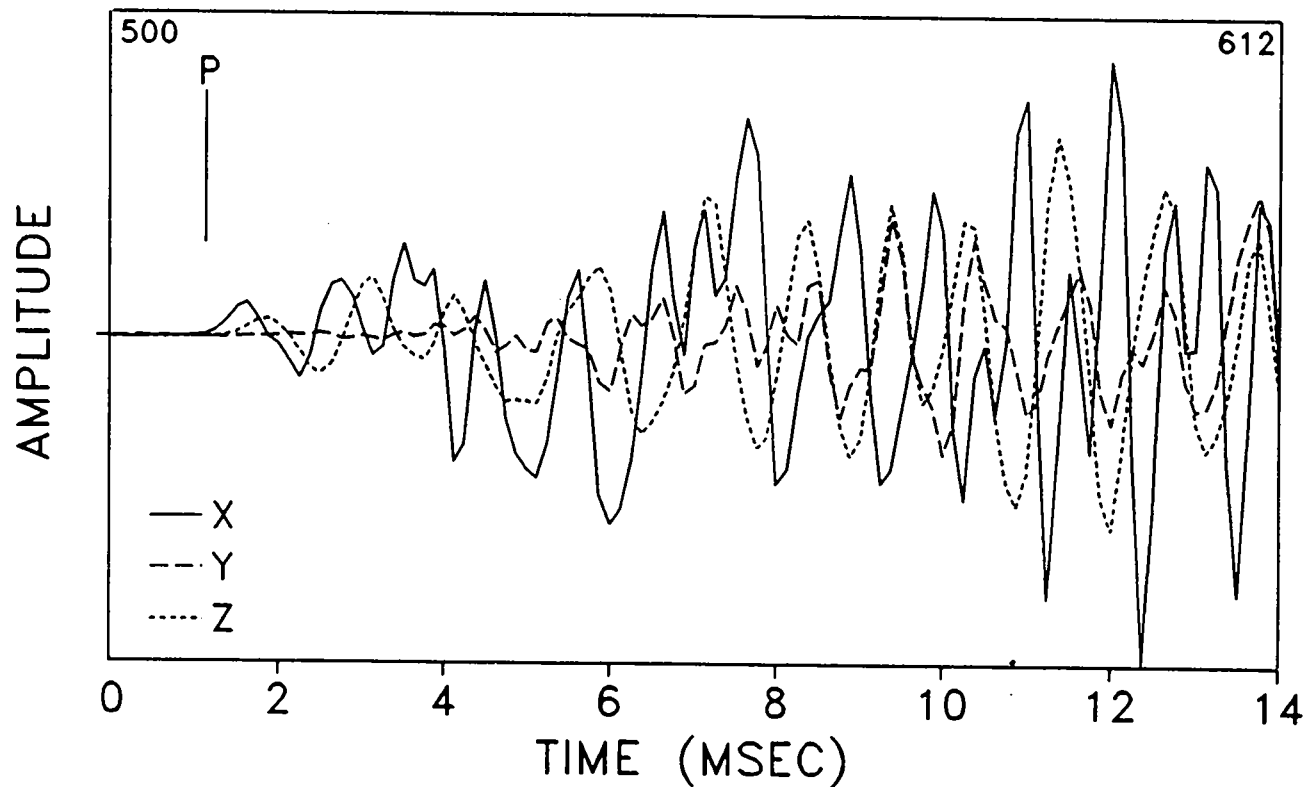
Time/Sec

ORIENTATION SCAN RESULTS



HODOGRAM
P: 509: 1.12 ms
TO 537: 4.63 ms

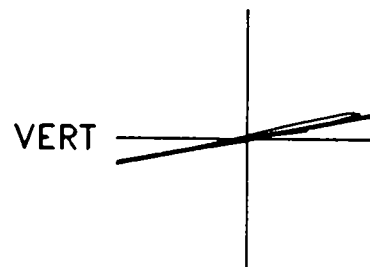
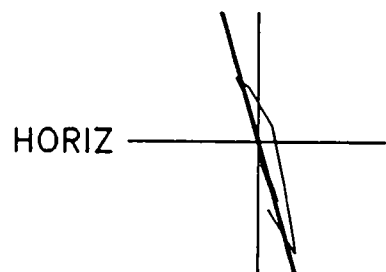
H: 0.5 SD: 11.1
V: -11.5 SD: 34.5
RMS H: 6.8 V: 27.4
VEL FAC: 22.3
DISTANCE: -1419



M-SITE MWX2
LEVEL 1
10/29/93
10299337.DAT
SCALE=20.8
SAMP INT:
0.125 ms
2049 PTS

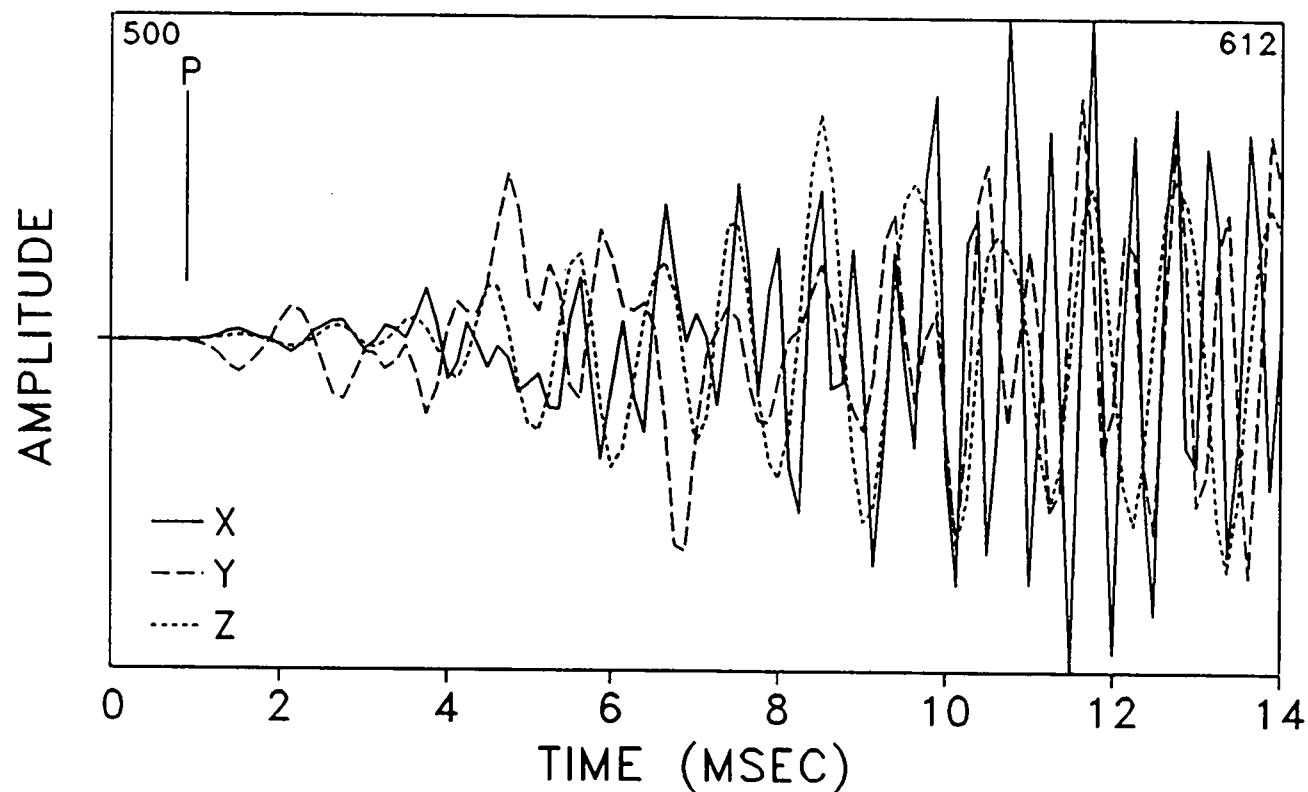
Figure 16. Example orientation data for level 1, shot at 4930 ft.

ORIENTATION SCAN RESULTS



HODOGRAM
P: 507: 0.88 ms
TO 525: 3.13 ms

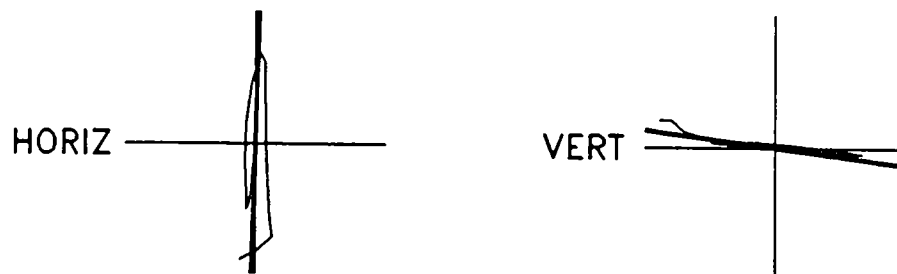
H: -74.0 SD: 10.5
V: 10.8 SD: 5.2
RMS H: 71.4 V: 14.8
VEL FAC: 22.3
DISTANCE: -1413



M-SITE MWX2
LEVEL 2
10/29/93
10299337.DAT
SCALE=30.0
SAMP INT:
0.125 ms
2049 PTS

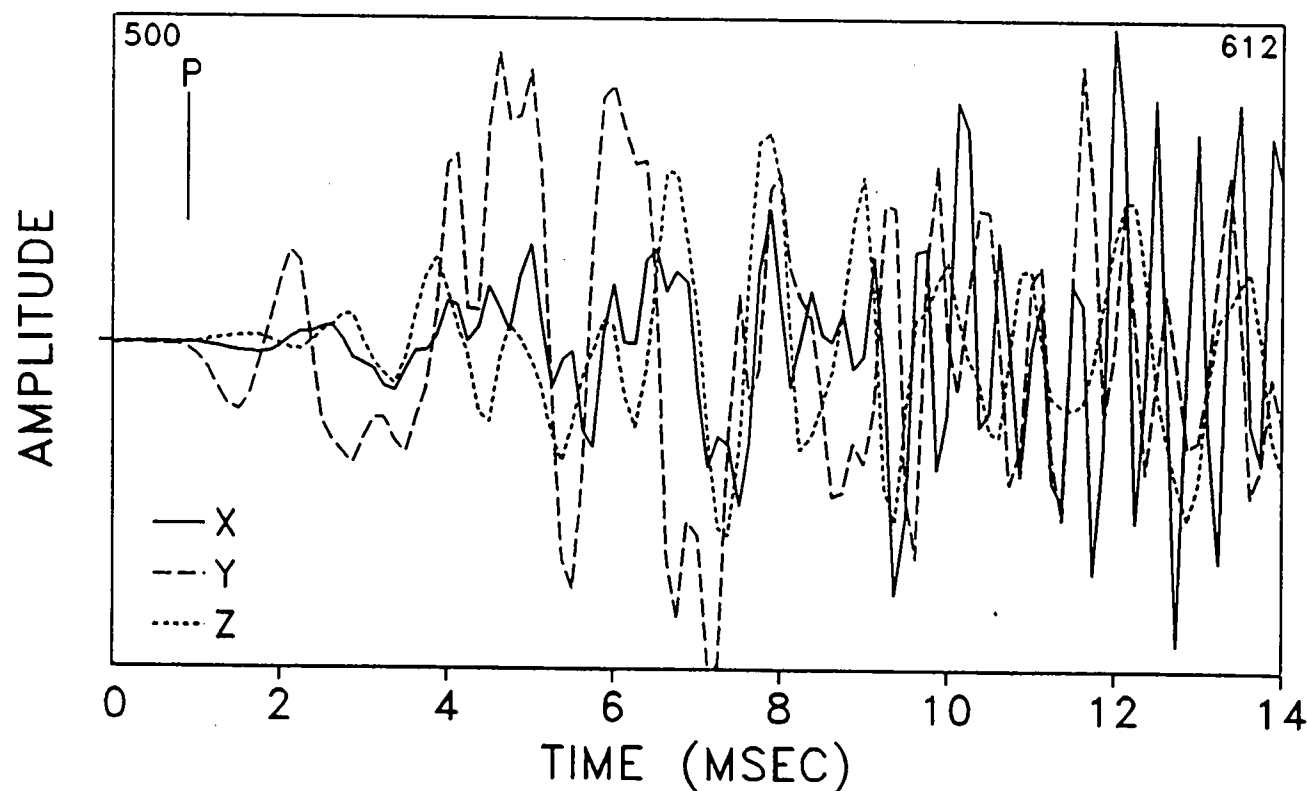
Figure 17. Example orientation data for level 2, shot at 4930 ft.

ORIENTATION SCAN RESULTS



HODOGRAM
P: 507: 0.88 ms
TO 525: 3.13 ms

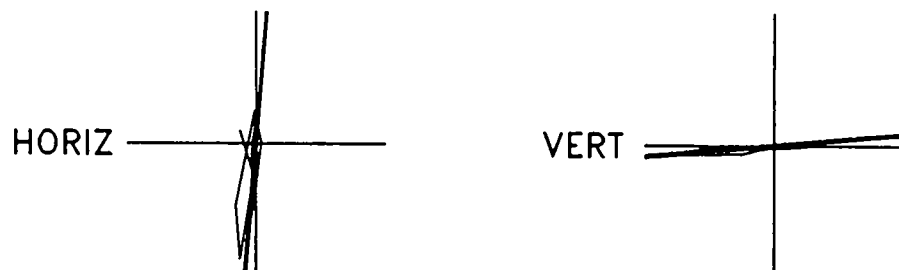
H: 88.3 SD: 10.7
V: -7.4 SD: 5.4
RMS H: 82.1 V: 9.8
VEL FAC: 22.3
DISTANCE: -1413



M-SITE MWX2
LEVEL 3
10/29/93
10299337.DAT
SCALE=18.7
SAMP INT:
0.125 ms
2049 PTS

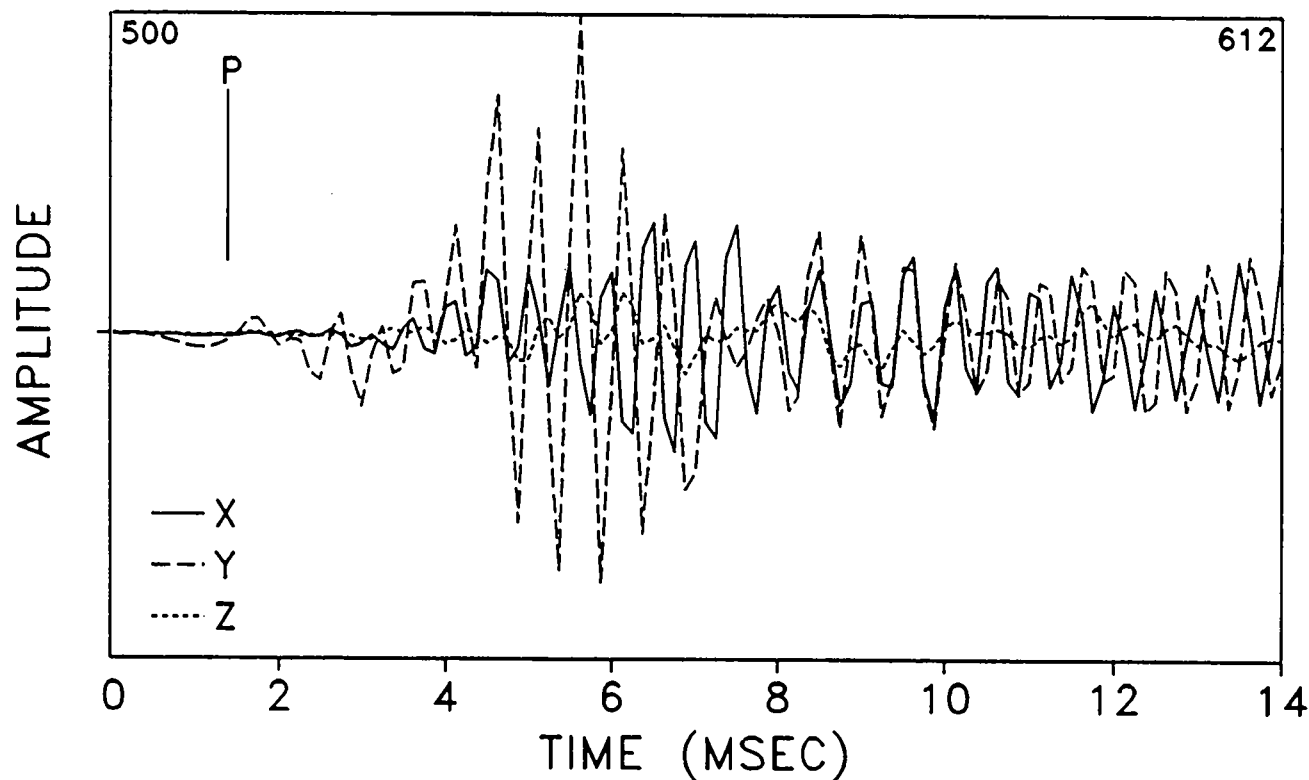
Figure 18. Example orientation data for level 3, shot at 4930 ft.

ORIENTATION SCAN RESULTS



HODOGRAM
P: 511: 1.37 ms
TO 528: 3.50 ms

H: 85.2 SD: 15.0
V: 4.9 SD: 6.2
RMS H: 79.2 V: 5.0
VEL FAC: 22.3
DISTANCE: -1424



M-SITE MWX2
LEVEL 4
10/29/93
10299337.DAT
SCALE=46.3
SAMP INT:
0.125 ms
2049 PTS

Figure 19. Example orientation data for level 4, shot at 4930 ft.

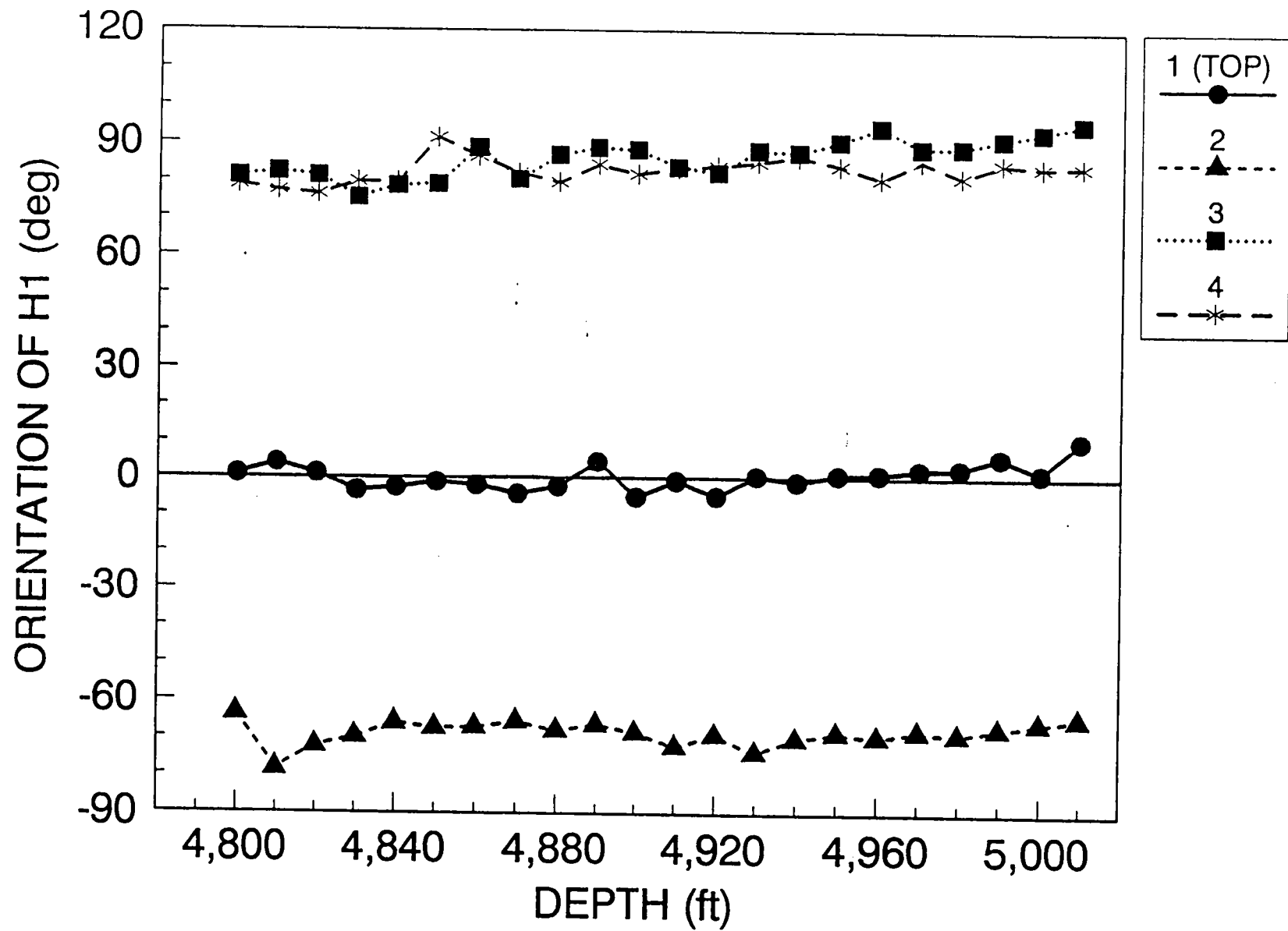
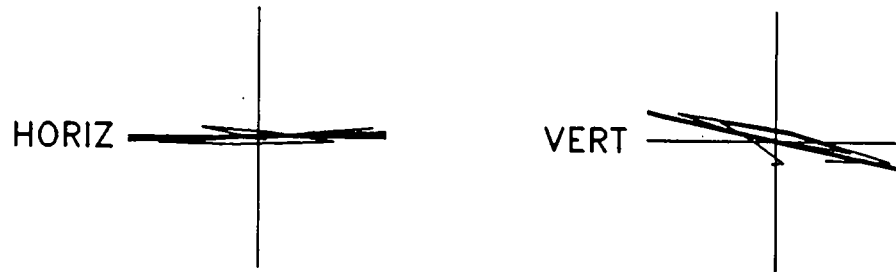
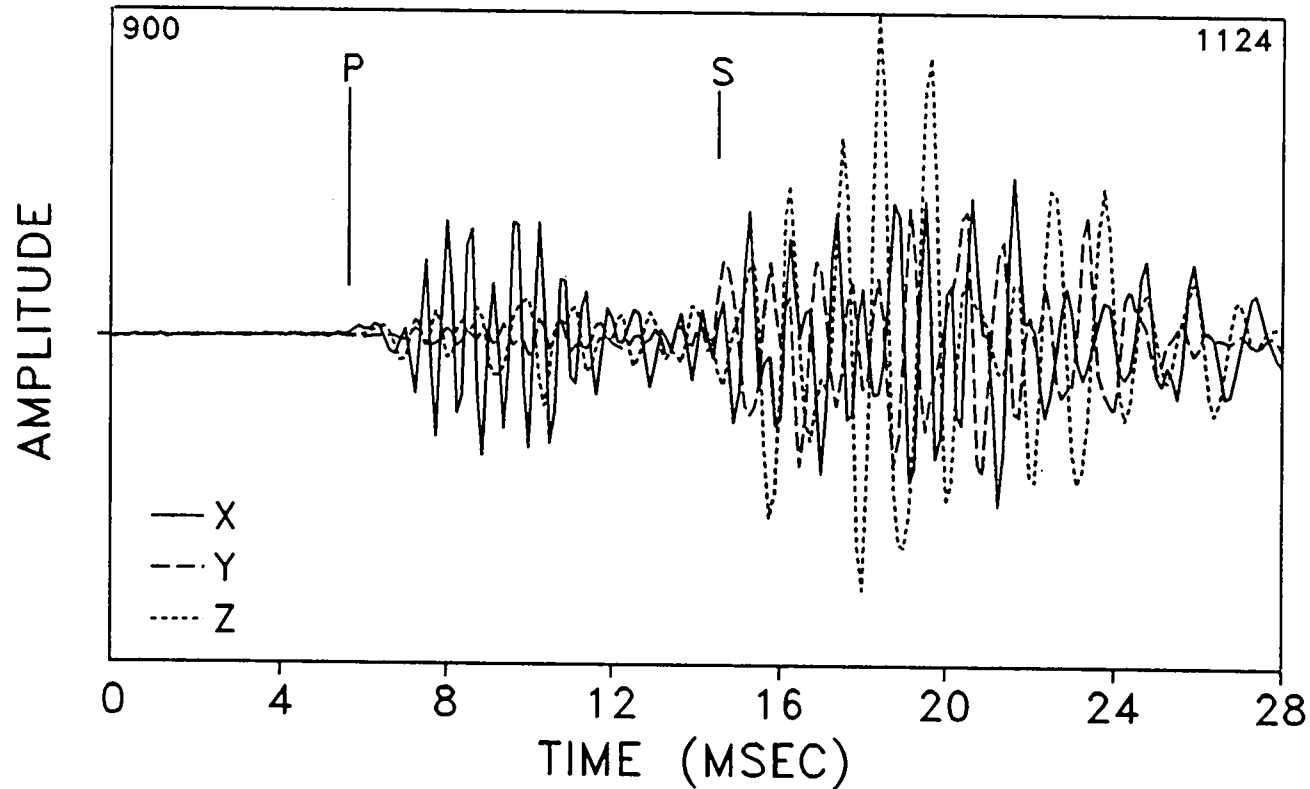


Figure 20. Orientation results for all levels.

FRACTURE #1 MICROSEISM



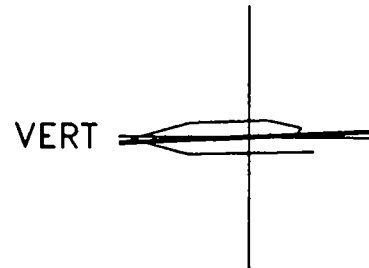
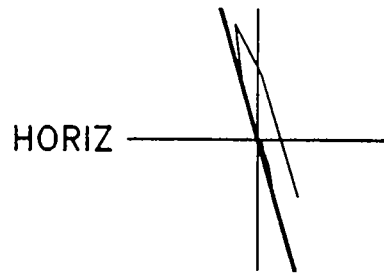
HODOGRAM
P: 945: 7.00 ms
RANGE 956: 5.63 ms
TO 967: 8.38 ms
S: 1016: 14.50 ms
H: 1.8 SD: 7.6
V: -12.0 SD: 20.2
RMS H: 5.7 V: 16.4
VEL FAC: 22.3
DISTANCE: 198



M-SITE MWX2
LEVEL 1
11/01/93
11019320.DAT
SCALE=5603.9
SAMP INT:
0.125 ms
2048 PTS

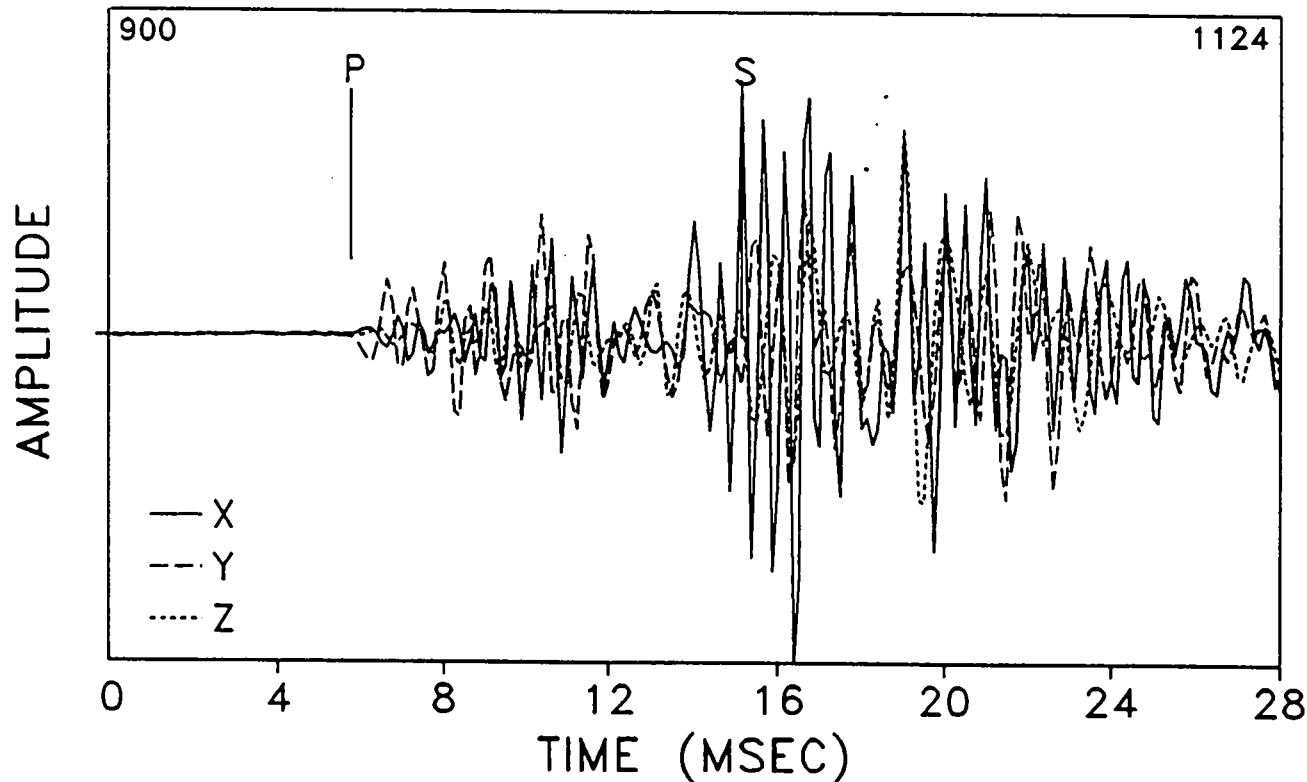
Figure 21. Example microseism data for level 1, microseism #20, frac #1.

FRACTURE #1 MICROSEISM



HODOGRAM

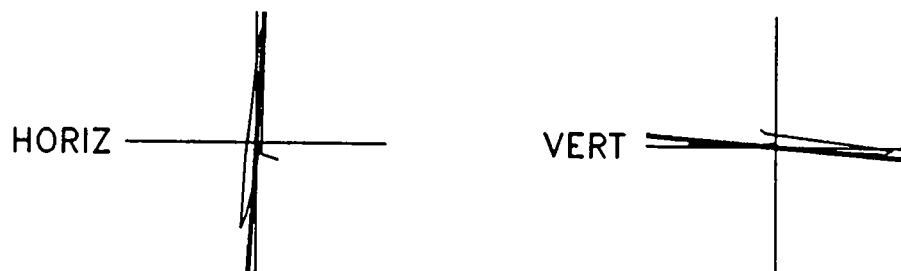
P: 946: 5.75 ms
 RANGE 946: 5.75 ms
 TO 957: 7.13 ms
 S: 1021: 15.13 ms
 H: -73.8 SD: 13.2
 V: 2.8 SD: 13.4
 RMS H: 72.0 V: 12.2
 VEL FAC: 22.3
 DISTANCE: 209



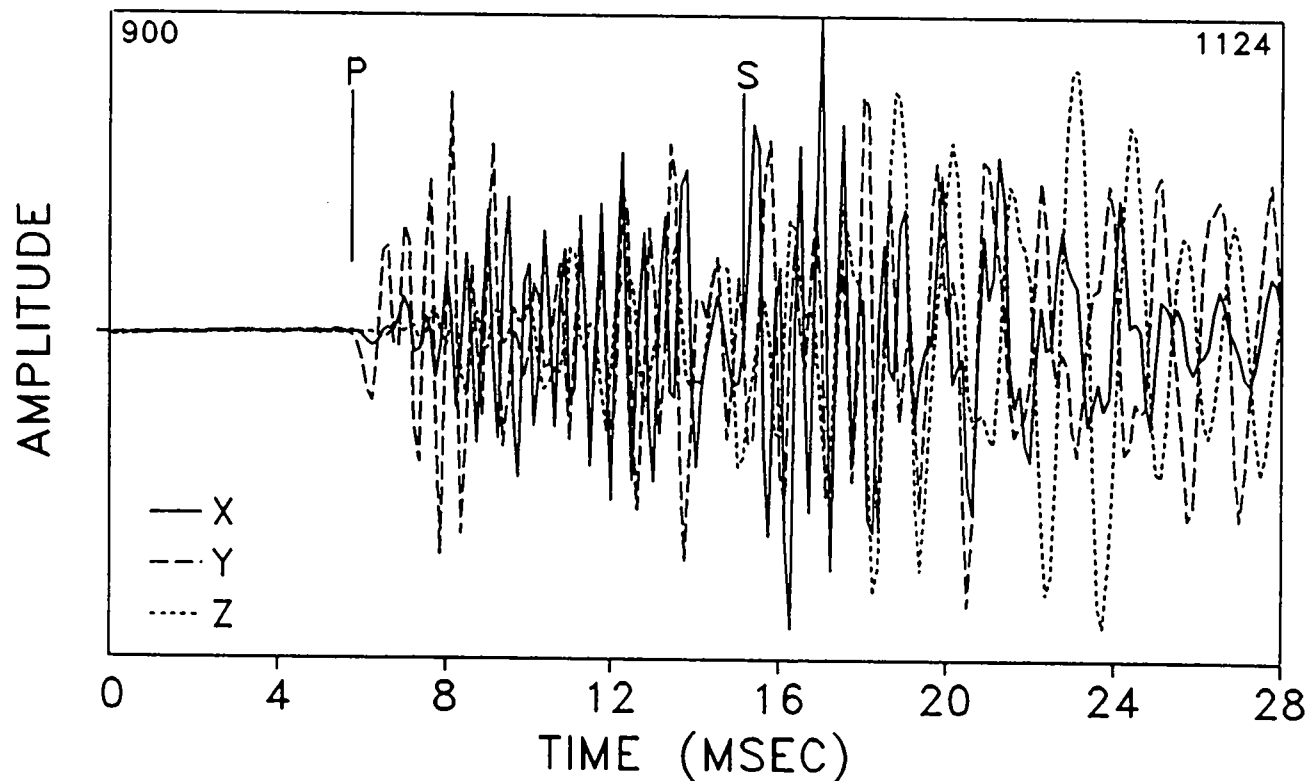
M-SITE MWX2
 LEVEL 2
 11/01/93
 11019320.DAT
 SCALE=6764.0
 SAMP INT:
 0.125 ms
 2048 PTS

Figure 22. Example microseism data for level 2, microseism #20, frac #1.

FRACTURE #1 MICROSEISM



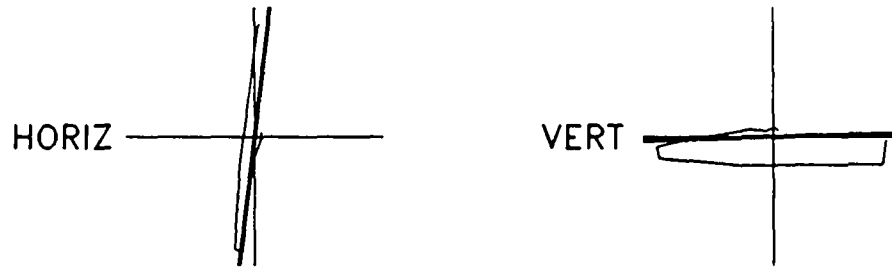
HODOGRAM
P: 946: 5.75 ms
RANGE 946: 5.75 ms
TO 957: 7.13 ms
S: 1021: 15.13 ms
H: 86.6 SD: 15.4
V: -4.8 SD: 13.9
RMS H: 80.8 V: 6.9
VEL FAC: 22.3
DISTANCE: 209



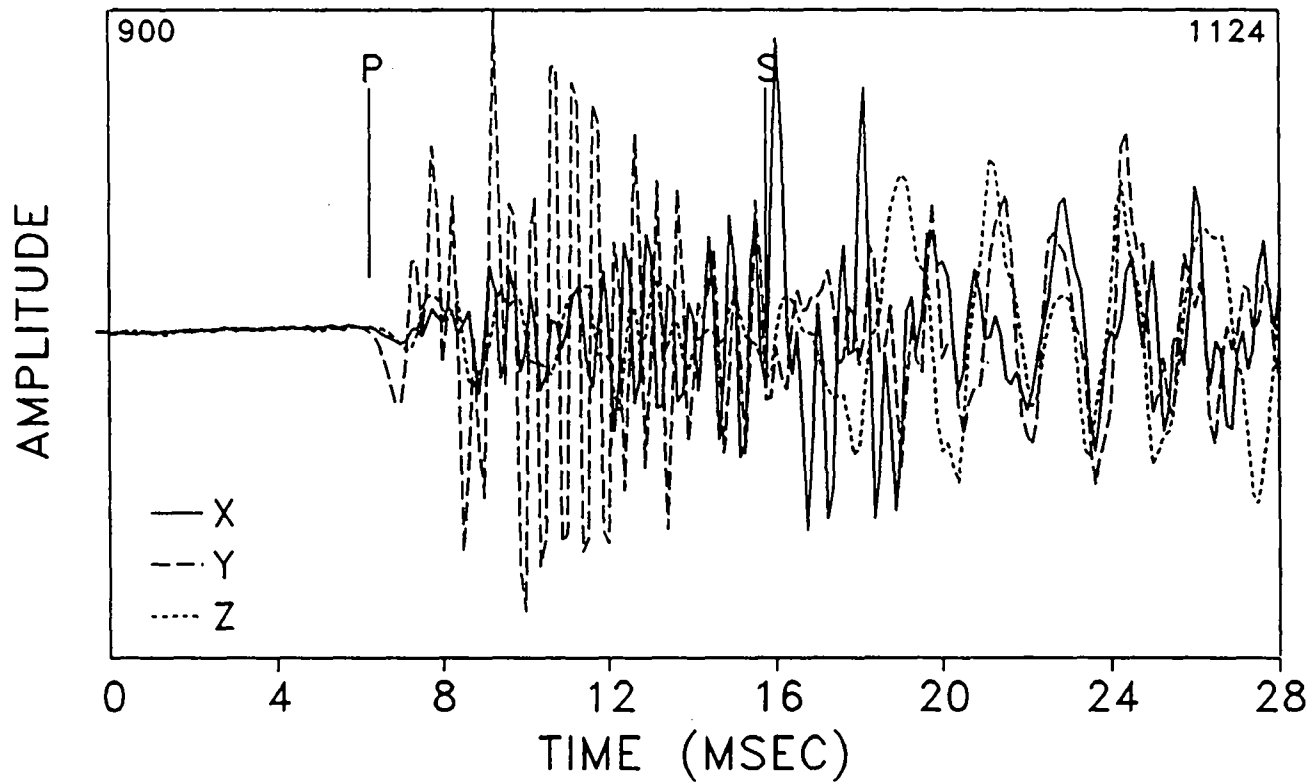
M-SITE MWX2
LEVEL 3
11/01/93
11019320.DAT
SCALE=4638.0
SAMP INT:
0.125 ms
2048 PTS

Figure 23. Example microseism data for level 3, microseism #20, frac #1.

FRACTURE #1 MICROSEISM



HODOGRAM
P: 950: 6.25 ms
RANGE 950: 6.25 ms
TO 961: 7.63 ms
S: 1026: 15.75 ms
H: 83.4 SD: 9.9
V: 1.8 SD: 16.1
RMS H: 82.5 V: 11.0
VEL FAC: 22.3
DISTANCE: 212



M-SITE MWX2
LEVEL 4
11/01/93
11019320.DAT
SCALE=2488.0
SAMP INT:
0.125 ms
2048 PTS

Figure 24. Example microseism data for level 4, microseism #20, frac #1.

M-SITE 1993 DIAGNOSTICS TEST: FRAC #1

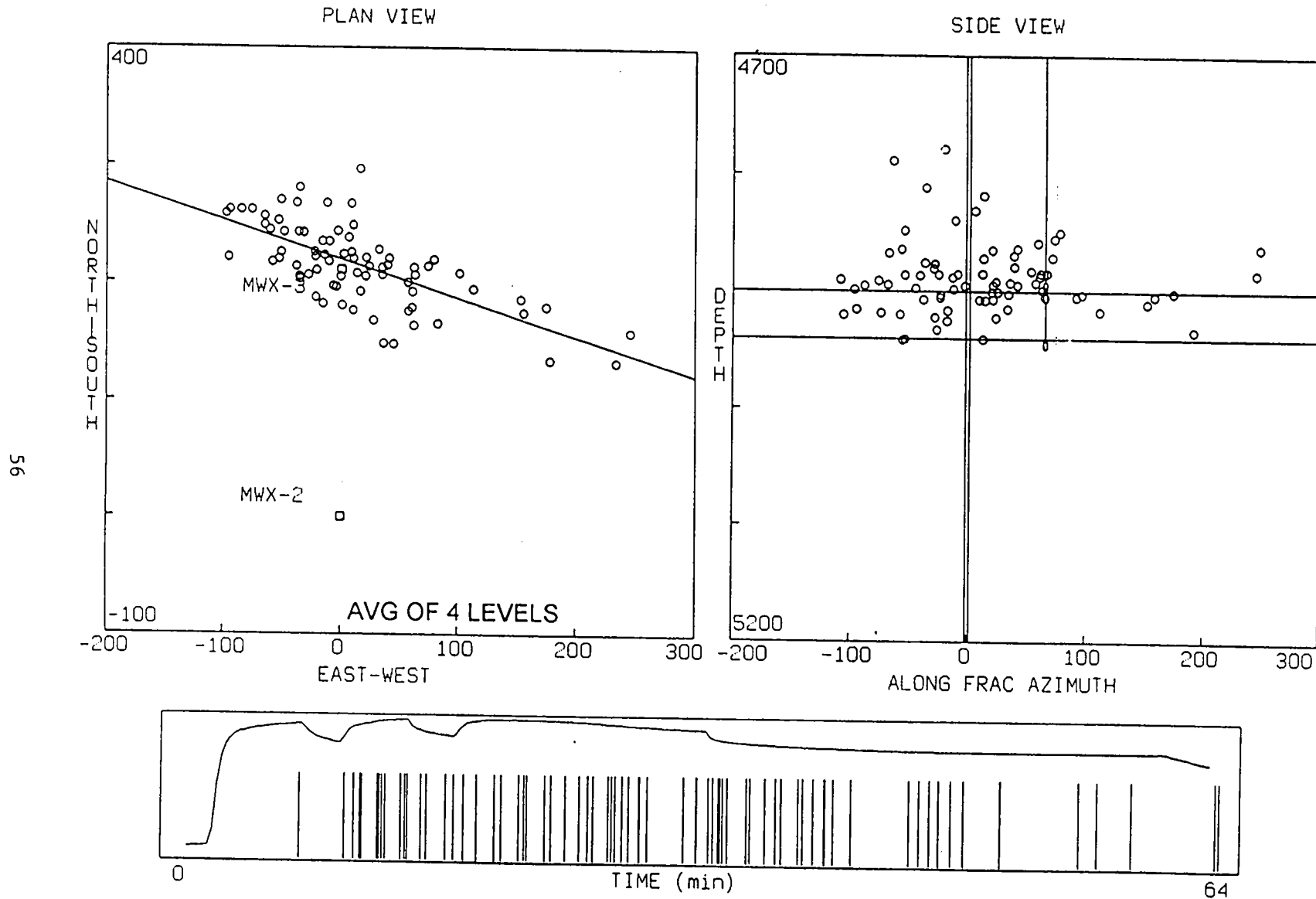


Figure 25. Initial map and histogram of frac #1 using unfiltered microseism data.